SEASONAL AND DECADAL-SCALE FORAGING HABITS OF THREE HAWAIIAN SEABIRDS

By

Kaycee Morra

A DISSERTATION

Submitted to
Michigan State University
In partial fulfillment of the requirements
for the degree of

Integrative Biology—Doctor of Philosophy

2018

ABSTRACT

SEASONAL AND DECADAL-SCALE FORAGING HABITS OF THREE HAWAIIAN SEABIRDS

By

Kaycee Morra

This dissertation describes three lines of investigation into the foraging habits of three pelagic seabirds using either whole tissue or amino acid-specific isotope data. First it asks whether information on foraging habits of the Hawaiian Petrel derived from isotope analysis of a primary feather grown at the beginning of the nonbreeding season (primary 1, P1) and in the middle of the nonbreeding season (primary 6, P6) is the same. Secondly, it compares long-term (greater than 50 years) foraging habits of Newell's shearwaters, Laysan albatross, and Hawaiian petrel using collagen-specific amino acid $\delta^{15}N$ proxies for nutrient regime and trophic position. Thirdly, it evaluates seasonal changes in modern Newell's shearwater and Laysan albatross foraging habits and, for Laysan albatross, extends this seasonal analysis back a century using collagen- and feather-specific amino acid $\delta^{15}N$ data.

Chapter one asked whether whole tissue isotope data for two feathers (P1 and P6) yielded similar information on the location and biogeochemical regime in which three colonies of Hawaiian petrel foraged. Relative to Hawaii and Lanai birds, the low P6 $\delta^{15}N$ values for Maui birds reflect foraging segregation and greater utilization of waters characterized by nitrogen fixation. There was no isotopic difference between P1 and P6, suggesting that either feather could be used to describe nonbreeding season foraging habits. This information increases our understanding of Hawaiian petrel foraging behavior over the nonbreeding season and informs sampling protocols for conservation managers who wish to understand nonbreeding season foraging.

Chapter two compared the foraging habits of modern and historical populations of three ecologically distinct species using amino acid-specific isotope analysis. The data show persistent inter- and intra-specific foraging segregation among Newell's shearwater, Laysan albatross, and two populations of Hawaiian petrel. While our nutrient proxy showed no shift in nutrient regime use over time, a significant trophic decline occurred for Newell's shearwater and Laysan albatross within the past century, paralleling a similar trend previously observed in the Hawaiian petrel. This builds on current evidence of a basin-wide shift in trophic dynamics within the North Pacific Ocean.

Chapter three uses amino acid-specific isotope analysis of feather and collagen to show that Newell's shearwater and Laysan albatross foraging habits (biogeochemical regime use and trophic position) differ between the breeding and nonbreeding seasons. In addition, within each season, each species utilizes a different foraging strategy despite the fact that they both breed on the Hawaiian Islands. While Laysan albatross have not altered their nonbreeding season foraging habits over the past century, the trophic decline they experienced occurred exclusively during the breeding season. Conservation management strategies for threatened seabirds like Newell's shearwater and Laysan albatross will require an understanding of at-sea risks—as well as threats on land—on seasonal timescales and may need to be individually tailored for each species.

.

This dissertation is dedicated to
my Mom, who reminds me daily how much I am loved;
my Dad, whose lack of concern for my future gives me confidence;
my Sister, who inspires me to be courageous and compassionate;
my Brother, whose strong character and gentle spirit comfort me.

ACKNOWLEDGEMENTS

I owe a debt of gratitude to countless individuals for their contributions to my dissertation work. In particular, I must thank the following people.

My doctoral advisor, Peggy Ostrom, for always striving toward what is best for my young career. Nathaniel Ostrom, for his thoughtful wisdom. Elise Zipkin and Sam Rossman for their statistical expertise, and Sam, for his willingness to teach me. My wonderful colleagues, Helen James and Anne Wiley, who always made time to offer considered and insightful feedback. Yoshito Chikaraishi, whose guidance was essential to my success in the lab. Hasand Gandhi, who regularly offered patience and expertise in the lab and smiles and calm company in the office.

The many conservationists and organizations working hard to protect our Hawaiian seabirds and support good research, including Cathleen Bailey, Jessie Beck, Megan Dalton, Fern DuVall, Shannon Fitzgerald, Michelle Hester, Darcy Hu, Robby Kohley, Kathleen Misajon, Hannah Nevins, Jay Penniman, Sheldon Plentovich, Andre Raine, Carl Schwarz, Eric Marie Van Zandt, VanderWerf, Bill Walker, Lindsay Young, The National Marine Fisheries Service, Alaska Fisheries Science Center, Pacific Islands Regional Office – Fisheries Observer Program staff and observers, the vessels and crews of the Hawaii longline fisheries that supported observers, Oikonos, the Hawaii Department of Land and Natural Resources, and the Kaua'i Endangered Seabird Recovery Project.

The Bird Division, National Museum of Natural History, the Bernice Bishop Museum—namely, Molly Hagemann, and the California Academy of Sciences for the loan of specimens and permission to sample them.

The many folks, like Jim, who kept the Natural Science building clean for all of us Spartans, particularly considering the countless nights they had to clean around me.

Finally, all my friends and loved ones who understood when I didn't have time, forgot, couldn't make it, or failed to remind them how appreciated they are.

TABLE OF CONTENTS

LIST OF TABLES

LIST OF FIGURES

INTRODUCTION

Among the tapestry of top predators that forage within the Pacific Ocean, seabirds are some of the most conspicuous and wide-ranging. Although pelagic seabirds are atypical in their dependence on a terrestrial breeding colony, they spend most of their lives navigating thousands of kilometers of open ocean. Since the 1950's, humans have become a top predator of the Pacific Ocean themselves and compete with seabirds, and other marine predators, for food. Scientists have recognized for decades that humans are in danger of overfishing some of the world's largest and most remote ecosystems, and fishers have noticed rapid and drastic declines in formerly abundant catches. By the time humans recognized they had underestimated the ocean's potential as a food source, they were dealing with the shocking realization that humans were capable of decimating such plentiful fish populations, potentially beyond recovery. Our understanding of fish stocks is often incomplete and is based on biased global marine catch statistics that offer little forewarning regarding fish abundances and distributions. Moreover, we have a limited understanding of how industrial-scale fish removal influences marine ecosystem integrity as a whole. As highly mobile top predators that occasionally become accessible on land, seabirds offer a unique opportunity to gain valuable insight into oceanic trophic dynamics. In addition to their potential to herald marine ecosystem change, their preserved tissues can provide a retrospective glimpse into a time that precedes catch statistics and inform long-term temporal shifts in oceanic food webs.

CHAPTER 1

Influence of Feather Selection and Sampling Protocol on Interpretations of Hawaiian Petrel (*Pterodroma sandwichensis*) Nonbreeding Season Foraging Habits from Stable Isotope Analysis

ABSTRACT

Isotope data from Hawaiian Petrel (*Pterodroma sandwichensis*) primaries P1 and P6 were compared to determine whether foraging habits change between the beginning and middle of the nonbreeding season. P6 data did not differ between samples derived from a longitudinal and a minimally invasive protocol and point samples taken from the feather bases. While P6 $\delta^{13}C$ increased longitudinally, no $\delta^{15}N$ longitudinal trends emerged, yet inter-individual $\delta^{15}N$ variability was high. P6 $\delta^{13}C$ data suggest that Hawaiian Petrels molt at low latitudes. Among colonies, all of which are located in the Hawaiian Islands, USA, low P6 $\delta^{15}N$ values for Maui birds relative to Hawaii and Lanai birds reflect foraging segregation and differential utilization of ^{15}N-enriched oceanic regions. For the Hawaiian Petrel, the isotopic similarity between P1 and P6 indicates that analogous ecological interpretations can be drawn from these feathers, and similar foraging habits persist from the beginning to middle of the nonbreeding season. Prolonged inter-colony foraging segregation may facilitate coexistence of colonies and, together with high intra-colony foraging diversity, may reduce extinction risk for the endangered Hawaiian Petrel.

INTRODUCTION

Remiges, retrices, coverts and contour feathers have been exploited for isotopic information that has advanced our understanding of avian foraging behavior (Navarro *et al*. 2009; Hinke *et al*. 2015; Cherel *et al*. 2016). Increasing concern that isotopically derived ecological inferences are dependent on feather type, molt timing and sampling protocol is problematic for conservation managers who sample live individuals (Edwards *et al*. 2015; Cherel *et al*. 2016). Moreover, sampling decisions are irreversible, emphasizing that careful consideration should be given to sampling protocols so that valuable resources are preserved for future research.

Our isotope approach is based on the observations that $\delta^{13}C$ values of phytoplankton and consumers vary inversely with latitude in the northern Pacific Ocean, and broad spatial gradients in $\delta^{15}N$ at the base of oceanic food webs are transferred to consumers with a systematic increase in $\delta^{15}N$ with trophic level (Graham *et al*. 2010). The Hawaiian Petrel (*Pterodroma sandwichensis*) is an excellent species in which to study isotopic variance among feathers because there are existing data on primary 1 (P1), and the timing and sequence of primary molt is well constrained (Wiley *et al*. 2010, 2012, 2013). Hawaiian Petrels, like other Procellariiformes, molt their primaries during the nonbreeding season (Pyle *et al*. 2011; Howell *et al*. 2012) and, like other species of the genera *Pterodroma*, their molt likely proceeds distally from the innermost to outermost primary, P1 to P10 (Warham 1996; Pyle 2008).

Because P1 likely grows over the first 12 to 35 days of the 3.5-6 month long nonbreeding season (Simons 1985), we questioned whether P1 adequately reflects post-breeding foraging behavior. Thus, we centered our current investigation on primary 6 (P6), which, based on estimates of feather growth rates in juvenile Hawaiian Petrels and other Procellariiformes, requires up to 100 days to grow (Sincock and Swedberg 1969; Ainley *et al*. 1976; Simons 1985)

and is grown later than P1. Our objectives were to determine whether $\delta^{13}C$ and $\delta^{15}N$ data from P1 and P6 provide similar information regarding nonbreeding season foraging, and to evaluate inter- and intra-feather variation. We analyzed birds from three colonies to examine whether ecological inferences were representative of the entire species.

METHODS

Study Area

Hawaiian Petrel feathers were acquired from carcasses salvaged from colonies on Hawaii, Lanai, and Maui islands, Hawaii, USA, between 1990 and 2008. Feathers were washed (87:13 v/v chloroform:methanol), rinsed with ultrapure distilled water (E-Pure, Barnstead), dried (25 °C), divided into 1-cm long sections and sampled according to one of three protocols. The rachis was excluded from analysis.

13-Section Protocol

Vanes from five P6 remiges were longitudinally divided into 13 1-cm sections and numbered from oldest (tip, 1) to youngest (base, 13) material (Fig. 1). Minor variations in length were accounted for by adjusting the size of section 13. Barbs were weighed and cut into 3-mm long fragments, and a 1.0-mg homogenized aliquot was used for $\delta^{13}C$ and $\delta^{15}N$ analysis. The mass-weighted isotope value of each aliquot was used to calculate whole feather isotope averages.

4-Section Protocol

The remaining homogenates from the five P6 remiges and an additional 26 P6 feathers were used for a 4-section protocol. 1.0-mg homogenates from the feather tip (sections 1 and 2 combined), the base (sections 12 and 13 combined), and mid-feather (sections 5 and 8, kept separate) were analyzed, and whole feather averages were calculated as described above (Fig. 1).

Barb-Sampling Protocol and Comparison of Protocols

Barbs from the base, middle, and tip of 31 P1 and 26 P6 remiges were combined into a single 1.0-mg sample from each feather for isotope analysis. The number of barbs from each section was based on the distribution of mass found in other Hawaiian Petrel P1 and P6 feathers. For P1, we combined barbs from sections 1, 4 and 7 (Wiley *et al*. 2010). For P6, we combined barbs from the tip (0.1 mg), section 5 (0.2 mg), section 8 (0.3 mg), and base (0.4 mg) (Fig. 1). We assessed whether our three sampling protocols yielded equivalent whole feather isotope values by first comparing the mass-weighted averages generated from the 13- and 4-section protocols. We then compared the 4-section and barb-sampling protocols.

Stable Isotope Analysis

Feather aliquots (1.0 mg) were analyzed with an elemental analyzer (Eurovector) interfaced to an Isoprime mass spectrometer (Elementar). Data are expressed in per mil (‰) as $\delta X = ([R_{sample}/R_{standard}]-1) \times 1{,}000$, where X is ^{13}C or ^{15}N, R is $^{13}C/^{12}C$ or $^{15}N/^{14}N$, and $R_{standard}$ is V-PDB and air for $\delta^{13}C$ and $\delta^{15}N$, respectively. Isotopically characterized muscle tissue standards were analyzed between every nine unknowns. Precision was < 0.2‰ for $\delta^{13}C$ and $\delta^{15}N$.

Statistical Analyses

Differences in isotope values between protocols and between P1 and P6 were evaluated with two-tailed paired t-tests. Data from the 4-section protocol were used to evaluate the effects of colony and feather section on isotope values with three-way ANOVA models. Tukey's honestly significant difference (HSD) tests were implemented to evaluate variation among colonies and feather sections. Normality and heteroscedasticity were checked with normal quantile-quantile plots and Levene's tests. To determine if isotope values of white bases and whole feather averages differed, we constructed Gaussian linear mixed effects models with isotope value as the

dependent variable, and colony and sample type (feather base, whole feather average) as factors. Individual was a random effect to account for individual variation. Statistical tests were completed in statistical package R (R Development Core Team 2016).

RESULTS

The 13-section protocol provided the most complete estimate of a feather's isotope value. The difference between the 4-section and 13-section protocol was analytically undetectable (≤ 0.1‰ for $\delta^{13}C$ and $\delta^{15}N$) and statistically insignificant (Table 1).

For all colonies, the difference between the barb-sampling and 4-section protocols was ≤ 0.4‰ for $\delta^{13}C$ and $\delta^{15}N$ and not statistically significant (Table 1). Although the 0.2‰ difference between $\delta^{13}C$ base and whole feather averages estimated by our mixed model was significant (Table 2), it was equal to our analytical error and not ecologically significant. $\delta^{15}N$ did not differ between bases and whole feather averages (Table 2). Paired P1 and P6 barb-sampling protocol data from 25 individuals (7 from Hawaii, 8 from Lanai, and 10 from Maui) showed no significant difference in $\delta^{13}C$ or $\delta^{15}N$ between P1 and P6 (Table 3).

For every colony and almost every individual, $\delta^{13}C$ values increased from tip to base, and feather section was a significant factor (Table 4; Fig. 2). P6 $\delta^{13}C$ was equivalent across all three colonies and not a function of individual (Table 4). P6 feather section pairs were significantly different in $\delta^{13}C$, except for the section 1 and 5 comparison (Tukey HSD $P > 0.05$).

There was no longitudinal trend in $\delta^{15}N$ for individuals or colonies, and feather section did not influence $\delta^{15}N$ values (Table 5; Fig. 3). $\delta^{15}N$ was a function of colony and individual (Table 5). There was no difference in P6 $\delta^{15}N$ between Lanai and Hawaii; however, Maui P6

$\delta^{15}N$ was the lowest of all colonies (Tukey HSD $P < 0.05$ and $P < 0.01$ for Hawaii and Lanai, respectively; Table 5).

DISCUSSION

Our investigation of Hawaiian Petrel primary feathers improved our understanding of how feather selection influences isotopically derived ecological inferences. Development of P6 sampling approaches was essential in delineating isotopic variability within feathers, identifying a minimally invasive sampling protocol, and stimulating considerations for sampling strategy. The sampling protocols used to characterize P6 whole feather averages avoid potential bias from point sampling and reflect the longest time period possible from a single feather. The minimally invasive barb-sampling protocol is relatively fast, reduces damage to museum specimens, and is unlikely to affect live bird flight ability. However, this protocol only produces a single average value for the feather. If evaluation of intra-feather isotope variation is desired, we recommend sampling along the length of the vane, similar to our 13- and 4-section protocols.

Data from our 4-section protocol characterized P6 $\delta^{13}C$ and $\delta^{15}N$ intra-feather variation. For P1, Wiley *et al.* (2010) had observed a tip to base increase in $\delta^{13}C$ values in the Hawaiian Petrel and Newell's Shearwater (*Puffinus newelli*), and a slight rise in Hawaiian Petrel $\delta^{15}N$. In our results, regardless of colony, the majority of P6 feathers exhibited a longitudinal increase in $\delta^{13}C$, similar to P1. None of the colonies exhibited a $\delta^{15}N$ longitudinal trend. Of 26 P6 feathers, only six had unidirectional $\delta^{15}N$ slopes along the length of the vanes; the remaining 20 exhibited various longitudinal $\delta^{15}N$ patterns.

Three factors could contribute to longitudinal isotopic increases: melanin pigmentation, fractionation associated with feather growth, and foraging behavior changes (Wiley *et al*. 2010).

However, isotope variation cannot be confounded by melanin or fractionation for white feather base point samples that lack melanin and are not differentially influenced by growth. The observation that isotope values of white bases and whole feather averages are similar indicates that inferences regarding differences in foraging behavior among individuals and colonies can be drawn from our data.

Foraging location is thought to drive $\delta^{13}C$ and $\delta^{15}N$ variation among seabirds (Wiley *et al*. 2010). Spatial variation in $\delta^{15}N$, rather than trophic level, is likely a dominant control of Hawaiian Petrel feather $\delta^{15}N$ (Wiley *et al*. 2013). Thus, P6 longitudinal isotopic variation and variation among individuals in P6 $\delta^{15}N$ likely relates to foraging location differences. Our $\delta^{13}C$ values are higher than those of seabirds that forage in the North Pacific Transition Zone (40 to 45° N) (Gould *et al*. 1997), suggesting that Hawaiian Petrels molt at more southerly latitudes than the Transition Zone birds. Observational records, tagging data, and P6 $\delta^{15}N$ data all indicate that Hawaiian Petrels forage at low latitudes post-breeding. Spear *et al*. (1995) observed Hawaiian Petrels southeast of Hawaii during the nonbreeding season, and tagging data show Lanai birds south of Hawaii post-breeding (VanZandt 2012). Differential foraging in a ^{15}N-enriched area southeast of Hawaii or in waters whose nutrients are ^{15}N depleted by nitrogen fixation may drive the inter-colony foraging segregation shown by P6 $\delta^{15}N$ data (Ostrom *et al*. 2017). Relative to Maui birds, Hawaii and Lanai birds likely have high P6 $\delta^{15}N$ values because they forage more in waters with elevated $\delta^{15}N$ during the nonbreeding season. Collagen amino acid $\delta^{15}N$ values also suggest that Hawaii and Maui colonies differ in foraging location (Ostrom *et al*. 2017).

An important objective was to determine whether P1 and P6 yield similar information on nonbreeding season foraging, when foraging habits are particularly difficult to ascertain. Given

that P1 and P6 do not differ isotopically, our results suggest that similar ecological information can be obtained from these feathers.

Our data fortify interpretations made by Wiley *et al*. (2012) regarding inter-colony foraging differences. Wiley *et al*. (2012) suggested that inter-colony foraging segregation may reflect niche partitioning driven by competition, and facilitate colony coexistence (Lewis *et al*. 2001; Navarro *et al*. 2009). The P6 results indicate that inter-colony differences observed at the onset of the nonbreeding season are protracted. Sustained foraging segregation during the nonbreeding season shows ecological diversity, an attribute that may reduce extinction risk for small populations. Similarly, foraging variation within each colony (i.e., $\geq$ 4‰ range in P6 average $\delta^{15}N$) may promote the viability of a small population.

For Hawaiian Petrels, sampling P6 offers advantages over P1; P6 is relatively distal, accessible and a viable option for species where molt timing and sequence are constrained. Some albatrosses simultaneously molt distally and proximally and vary the extent of molt annually (Edwards and Rohwer 2005). In such cases, feather selection must be deliberated with regard to the time over which foraging habits are recorded. While non-pigmented point samples avoid pigmentation-associated isotopic variance, whole feather averages reflect a longer timeframe but require more handling than point samples. Importantly, it may be difficult to dismiss pigmentation as a confounding factor for feathers with a complicated pigmentation pattern.

Isotopic inferences made from P1 and P6 suggest that foraging segregation between Hawaiian Petrel colonies persists into the heart of the nonbreeding season, that there is large variation among individuals in foraging location, and that molt likely takes place at low latitudes. Our results strengthen evidence that Hawaiian Petrels breeding on different Hawaiian islands are ecologically distinct (Wiley *et al*. 2012). Additional efforts including a well-considered study of

individual specialization and additional amino acid isotope analyses will be important future contributions to understand Hawaiian Petrel at-sea ecology.

APPENDIX

Figure 1. Schematic for Hawaiian Petrel primary 6 feather sampling protocols. Solid lines depict the division of the vanes into 13 1-cm sections (labeled 1-13) and dashed lines indicate the locations of barbs sampled in the barb-sampling protocol. Shading indicates sections that were homogenized and analyzed in the 13- and 4-section protocols. (A) 13-section protocol; each section was homogenized and subsampled for stable-isotope analysis. (B) The 4-section protocol; sections 1 and 2, 5, 8, and 12 and 13 were homogenized and sub-sampled. (C) Barb-sampling protocol; barbs from the border of sections 1 and 2 and 12 and 13 and barbs from the centers of sections 5 and 8 were combined to form a sample for isotope analysis.

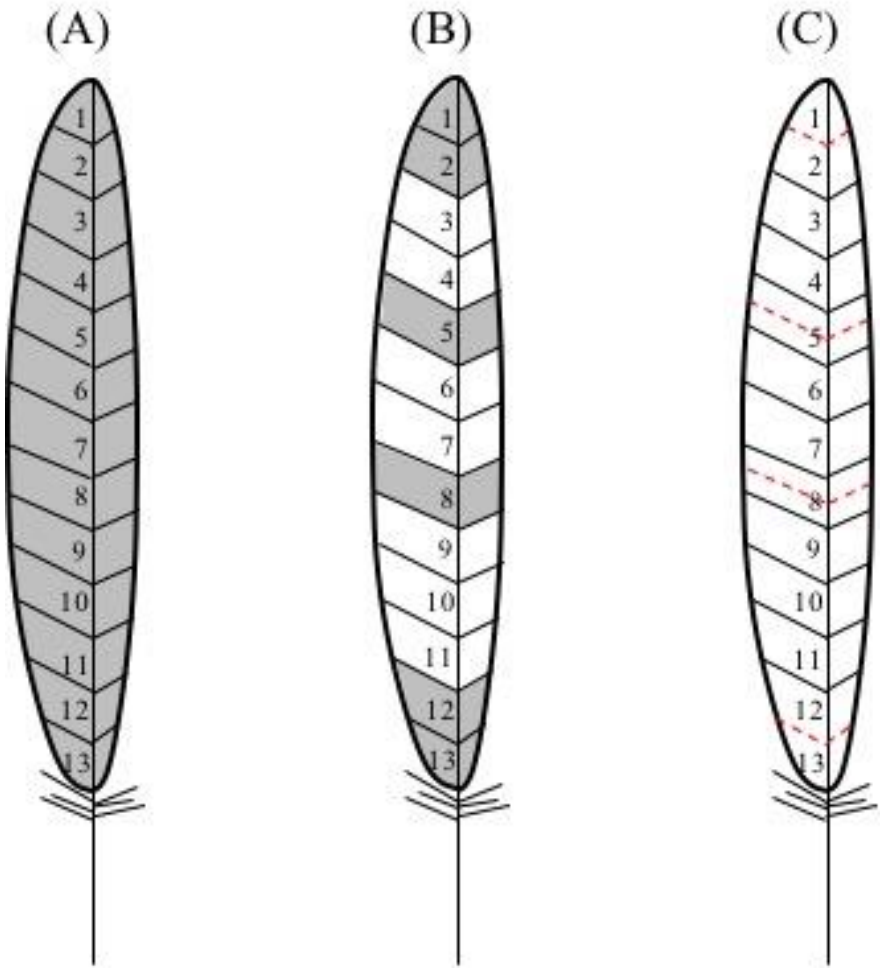

Figure 2. Longitudinal $\delta^{13}C$ values for Hawaiian Petrel primary 6 (P6) feathers obtained from the 4-section protocol. Data progress from section 1 (tip) on left to section 13 (base) on right. (A) Longitudinal trends in $\delta^{13}C$ for individuals. (B) Average $\delta^{13}C$ (standard deviation) for each feather section from three colonies. Line style indicates breeding colony: red solid = Hawaii, green dashed = Lanai, blue dash-dot = Maui.

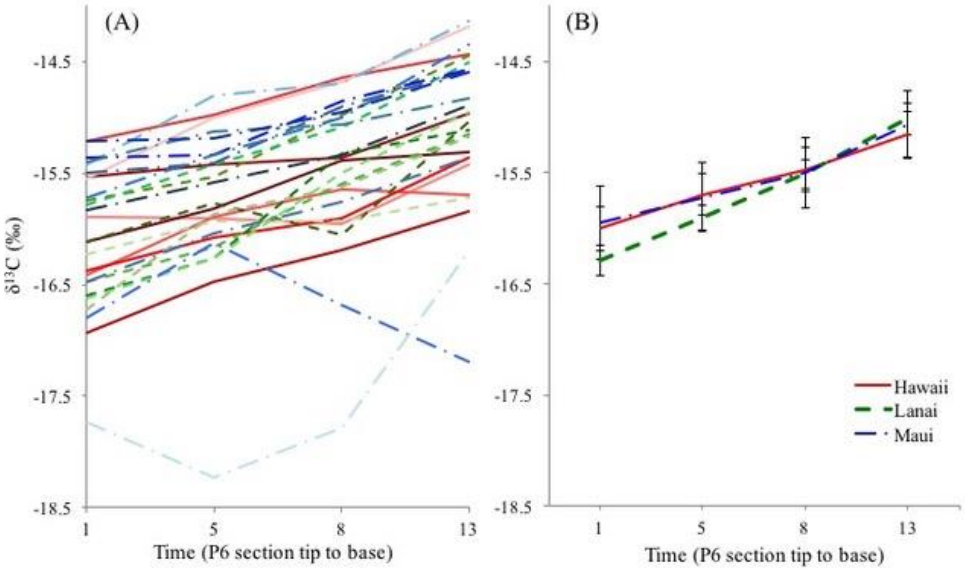

Figure 3. Longitudinal $\delta^{15}N$ values for Hawaiian Petrel primary 6 (P6) feathers obtained from the 4-section protocol. Data progress from section 1 (tip) on left to section 13 (base) on right. (A) Longitudinal trends in $\delta^{15}N$ for individuals. (B) Average $\delta^{15}N$ (standard deviation) for each feather section from three colonies. Line style indicates breeding colony: red solid = Hawaii, green dashed = Lanai, blue dash-dot = Maui.

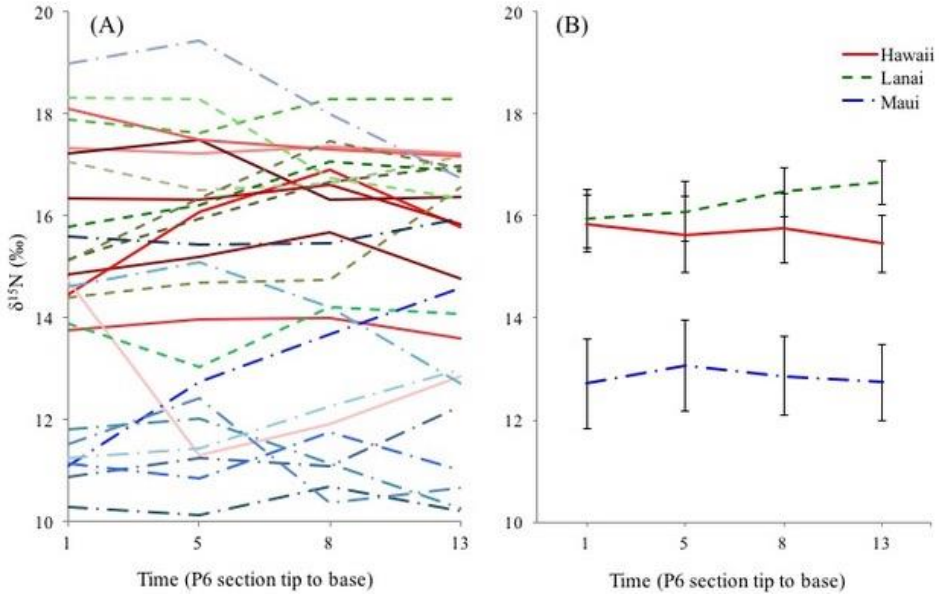

Table 1. Average difference (reported as absolute values) and standard deviation (SD) in $\delta^{13}C$ and $\delta^{15}N$ between Hawaiian Petrel primary 6 feather 13-section (13S), 4-section (4S), and barb-sampling (Barb) protocols, and results of paired t-tests (*P* values). Average differences are reported as absolute values. Data are from the islands of Hawaii, USA (Hawaii, Lanai and Maui islands).

		$\delta^{13}C$ (‰)		$\delta^{15}N$ (‰)	
Sampling Protocol	Sample Size	Average Difference (SD)	*P*	Average Difference (SD)	*P*
13S vs. 4S (Lanai, Maui)	5	0.0 (0.2)	0.90	0.1 (0.5)	0.60
4S vs. Barb (Hawaii)	8	0.1 (0.2)	0.10	0.0 (0.2)	0.70
4S vs. Barb (Lanai)	8	0.0 (0.1)	0.60	0.2 (0.4)	0.20
4S vs. Barb (Maui)	10	0.2 (0.5)	0.30	0.4 (0.9)	0.20

Table 2. Parameter estimates (Est) from linear mixed models of primary 6 base and whole feather $\delta^{13}C$ and $\delta^{15}N$ values with colony and sample type included as fixed effects and individual (Indiv) included as a random effect. Estimates are relative to the reference colony Hawaii and sample type whole feather. The model used restricted maximum likelihood t-tests with Satterthwaite approximations to degrees of freedom. SD = standard deviation; SE = standard error; Var = variance. Significant *P* values are indicated with an asterisk.

	$\delta^{13}C$ (‰)					$\delta^{15}N$ (‰)				
Fixed Effects	Est	SE	df	*t*	*P*	Est	SE	df	*t*	*P*
Intercept	-15.40	0.24	24	-64.10	< 0.001*	15.60	0.68	32	23.00	< 0.001*
Colony Lanai	-0.09	0.34	24	-0.25	0.80	0.62	0.89	32	0.70	0.49
Colony Maui	0.01	0.32	24	0.03	0.98	-2.78	0.87	32	-3.19	0.003*
Sample Type Base	0.22	0.08	23	2.81	0.01*	-0.13	0.32	28	-0.40	0.69
Random Effect		Var		SD			Var		SD	
Indiv		0.44		0.66			3.25		1.80	
Residual		0.03		0.16			0.42		0.65	

Table 3. Average difference (reported as absolute values) and standard deviation (SD) in $\delta^{13}C$ and $\delta^{15}N$ between primary feathers 1 and 6 of Hawaiian Petrels from three colonies (Hawaii, Lanai, and Maui islands), sample sizes and results of paired t-tests (*P* values). Data were obtained using the barb-sampling protocol.

		$\delta^{13}C$ (‰)		$\delta^{15}N$ (‰)	
Colony	Sample Size	Average Difference (SD) between P1 and P6	*P*	Average Difference (SD) between P1 and P6	*P*
Hawaii	7	0.2 (0.3)	0.10	0.2 (1.7)	0.80
Lanai	8	0.2 (0.3)	0.10	1.8 (1.7)	0.10
Maui	10	0.3 (0.5)	0.10	0.7 (1.8)	0.30

Table 4. Results of a three-way ANOVA model where $\delta^{13}C$ values are a function of individuals, breeding island and/or primary 6 feather section. The three-way ANOVA model was based on data from the 4-section protocol. Significant *P* values are indicated with an asterisk.

Model	*F*	*P*
Individual	1.182	0.28
Colony	1.140	0.29
Feather Section	30.670	< 0.05*
Individual + Colony	0.586	0.45
Individual + Feather Section	0.716	0.40
Colony + Feather Section	0.461	0.50
Individual + Colony + Feather Section	0.090	0.77

Table 5. Results of a three-way ANOVA model where $\delta^{15}N$ values are a function of individuals, breeding colony and/or primary 6 feather section. The three-way ANOVA model was based on data from the 4-section protocol. Significant *P* values are indicated with an asterisk.

Model	*F*	*P*
Individual	9.699	< 0.05*
Colony	21.670	< 0.05*
Feather Section	0.037	0.85
Individual + Colony	0.714	0.40
Individual + Feather Section	0.050	0.82
Colony + Feather Section	0.148	0.70
Individual + Colony + Feather Section	1.090	0.30

LITERATURE CITED

LITERATURE CITED

Ainley DG, Lewis TJ, Morrell S. 1976 Molt in Leach's and Ashy Storm-Petrels. Wilson Bull. 88: 76-95.

Cherel YP Quillfeldt KD, Weimerskirch H. 2016 Combination of at-sea activity, geolocation and feather stable isotopes documents where and when seabirds molt. Front. Ecol. Evol. 4: 3.

Edwards AE, Rohwer S. 2005 Large-scale patterns of molt activation in the flight feathers of two albatross species. Condor 107: 835-848.

Edwards AE, Fitzgerald SM, Parrish JK, Klavitter JL, Romano MD. 2015 Foraging strategies of Laysan Albatross inferred from stable isotopes: implications for association with fisheries. PLoS One 10: e0133471.

Gould P, Walker W, Ostrom P. 1997 Foods of northern fulmars associated with high-seas drift nets in the transitional region of the North Pacific. Northwest. Nat. 78: 57-61.

Graham BS, Koch PL, Newsome SD, McMahon KW, Aurioles D. 2010 Using isoscapes to trace the movements and foraging behavior of top predators in oceanic ecosystems. In: West JB, Bowen GJ, Dawson TE, Tu KP (eds) Isoscapes: Understanding Movement, Pattern, and Process on Earth Through Isotope Mapping. Springer Science, Dordrecht, The Netherlands, pp 299-318.

Hinke JT, Polito MJ, Goebel ME, Jarvis S, Reiss CS, Thorrold SR, Trivelpiece WZ, Watters GM. 2015 Spatial and isotopic niche partitioning during winter in chinstrap and Adélie penguins from the South Shetland Islands. Ecosphere 6: 1-32.

Howell, SNG, Patteson JB, Shearwater D. 2012 Petrels, albatrosses, and storm-petrels of North America: a photographic guide. Princeton University Press, Princeton, New Jersey.

Lewis S, Sherratt TN, Hamer KC, Wanless S. 2001 Evidence of intra-specific competition for food in a pelagic seabird. Nat. 412: 816-819.

Navarro J, Forero M, Gonzalez-Solis J, Igaul JM, Becares J, Hobson K. 2009 Foraging segregation between two closely related shearwaters breeding in sympatry. Biol. Lett. 5: 545-548.

Ostrom PH, Wiley AE, James HF, Rossman S, Walker WA, Zipkin EZ, Chikaraishi Y. 2017 Broad-scale trophic shift in the pelagic North Pacific revealed by an oceanic seabird. Proc. R. Soc. B: Biol. Sci. 284: 20162436-20162442.

Pyle P. 2008 Molt and age determination in Procellariiformes. Pages 248-260 *in* Identification Guide to North American Birds. Part 2: Anatidae to Alcidae. Slate Creek Press, Point Reyes Station, California.

Pyle P, Webster DL, Baird RW. 2011 Notes on petrels of the Dark-rumped Petrel complex (*Pterodroma phaeopygia/sandwichensis*) in Hawaiian waters. North Am. Birds 65: 364-367.

R Development Core Team. 2016 R: a language and environment for statistical computing v. 3.3.2. R Foundation for Statistical Computing, Vienna, Austria. http://www.R-project.org/, accessed 14 November 2016.

Simons TR. 1985 Biology and behavior of the endangered Hawaiian Dark-rumped Petrel. Condor 87: 229-245.

Sincock JL, Swedberg GE. 1969 Rediscovery of the nesting grounds of Newell's Manx Shearwater (*Puffinus puffinus newelli*), with initial observations. Condor 71: 69-71.

Spear LB, Ainley DG, Nur N, Howell SNG. 1995 Population size and factors affecting at-sea distributions of four endangered Procellariids in the tropical Pacific. Condor 97: 613-638.

VanZandt ML. 2012 Distribution and habitat selection of the endangered Hawaiian Petrel (*Pterodroma sandwichensis*), from the island of Lāna'i. PhD dissertation, University of Hawaii, Hilo.

Warham J. 1996 The behavior, population biology and physiology of the petrels. Academic Press, University of Canterbury, Christchurch, New Zealand.

Wiley AE, Ostrom PH, Stricker CA, James HF, Gandhi H. 2010 Isotopic characterization of flight feathers in two pelagic seabirds: sampling strategies for ecological studies. Condor 112: 337-346.

Wiley AE, Welch AJ, Ostrom PH, James HF, Stricker CA, Fleischer RC, Gandhi H, Adams J, Ainley DG, Duvall F, Holmes N. 2012 Foraging segregation and genetic divergence between geographically proximate colonies of a highly mobile seabird. Oecologia 168: 119-130.

Wiley AE, Ostrom PH, Welch AJ, Fleischer RC, Gandhi H, Southon JR, Stafford Jr. TR, Penniman JF, Hu D, Duvall FP, James HF. 2013 Millennial-scale isotope records from a wide-ranging predator show evidence of recent human impact to oceanic food webs. Proc. Natl. Acad. Sci. 110: 8972-8977.

CHAPTER 2

Trophic Declines and Decadal-Scale Foraging Segregation in Three Pelagic Seabirds

ABSTRACT

Oceanic ecosystems contain critical resources for humans but are increasingly at risk. Isotope values of wide-ranging seabirds offer an avenue to assess vast, remote ocean ecosystems. We investigate the foraging habits of Newell's shearwater (*Puffinus newelli*) and Laysan albatross (*Phoebastria immutabilis*) over the past 50 to 100 years, respectively, using amino acid $\delta^{15}N$ proxies for nutrient regime and tropic position. We compare these data to those published for the Hawaiian petrel (*Pterodroma sandwichensis*). Standard ellipses constructed from the isotope proxies show that Newell's shearwater, Laysan albatross and the Hawaiian petrel exhibit inter-population and interspecific foraging segregation that has persisted for several decades. We found no evidence of a shift in nutrient regime used by our study species. However, a significant trophic decline occurred during the past century for Newell's shearwater and Laysan albatross (probability ≥ 0.97), echoing a similar trend observed in the Hawaiian petrel. Because our study species are broadly distributed across the North Pacific Ocean, employ distinct feeding strategies and exhibit several other divergent morphological and behavioral traits, the trophic decline suggests a pervasive shift in food web architecture within the past century, most conceivably in response to industrial fishing.

INTRODUCTION

Vast remote open oceans, beyond the continental shelves, are of great economic and social importance (Costanza 1999). Unique insight into oceanic ecosystems can be obtained by studying wide-ranging top predators, including seabirds. Pelagic seabirds are particularly useful indicators of ecosystem change because they integrate molecular information on trophic dynamics and biogeochemical regimes in their body tissues as they forage over large oceanic expanses (Bearhop et al. 2006; Hinke et al. 2015). This information can be accessed through stable isotope analysis of those tissues.

The use of nitrogen isotopes to delineate trophic relationships has a long history (DeNiro and Epstein 1981; Minagawa and Wada 1984) built on observations of a systematic increase of ~3-4 ‰ in $\delta^{15}N$ with each trophic transfer (DeNiro and Epstein 1981; Minagawa and Wada 1984). A challenge lies in the recognition that whole tissue $\delta^{15}N$ values respond to both trophic level and source nitrogen supplied to the base of the food web. Compound specific nitrogen isotope analysis is able to disentangle these effects (Gaebler et al. 1963; McClelland and Montoya 2002; Chikaraishi et al. 2007; McMahon and McCarthy 2016; Ohkouchi et al. 2017). The $\delta^{15}N$ of "trophic" amino acids, such as glutamic acid ($\delta^{15}N_{Glu}$), becomes ^{15}N-enriched with increasing trophic level. This isotopic fractionation occurs during deamination and other metabolic reactions involving nitrogen transformation. The $\delta^{15}N$ of "source" amino acids, such as phenylalanine ($\delta^{15}N_{Phe}$), fractionates to a smaller degree with each trophic transfer. Consequently, $\delta^{15}N_{Phe}$ primarily reflects the isotope value of source nitrogen at the base of the food web, and as such, can be used as a nutrient proxy. The difference between the $\delta^{15}N_{Glu}$ and $\delta^{15}N_{Phe}$ of a consumer is a trophic proxy ($\Delta\delta^{15}N_{Glu\text{-}Phe}$) and is used to calculate trophic position (TP): $TP = (\delta^{15}N_{Glu} - \delta^{15}N_{Phe} - \beta)/TDF + 1$, where β is the $\delta^{15}N_{Glu} - \delta^{15}N_{Phe}$ difference in primary

producers and TDF is the trophic discrimination factor, or the net elevation of $\delta^{15}N_{Glu}$ relative to $\delta^{15}N_{Phe}$ per trophic step (McMahon and McCarthy 2016).

$\delta^{15}N_{Phe}$ from seabirds is useful because the $\delta^{15}N$ of source nitrogen varies across the Pacific Ocean. For example, there is an isotopic gradient southeast of the Hawaiian Islands with a conspicuous localized region of ^{15}N-enriched waters (4-10 °N and 135-140 °W) (Fig. 4; Altabet and Francois 1994; Graham et al. 2010). Such $\delta^{15}N$ gradients result from the prevalence of different biogeochemical processes. The $\delta^{15}N$ of the primary nitrogen source of oceans, nitrate, is 5-6 ‰ and becomes elevated due to denitrification and phytoplankton uptake (Karl et al. 1997; Sigman et al. 2000). Nitrogen fixation produces ammonium with $\delta^{15}N$ values of 0 ‰ (Karl et al. 1997; Casciotti et al. 2008). Because the $\delta^{15}N$ at the base of the food web is transferred to consumers, $\delta^{15}N_{Phe}$ values identify the biogeochemical regime in which seabirds forage.

Spatial variation in nitrogen added to or removed from the ocean by biogeochemical processes is identified as N*. N* refers to the excess or deficit in nitrogen (N) relative to phosphorus (P) from the expected Redfield N:P stoichiometry of 16:1, where $N^* = N - 16P + 2.9$ μmol kg^{-1} (Deutsch et al. 2001). Whereas average marine nitrate corresponds to an N* of 0, nitrogen fixation and denitrification both alter Redfield stoichiometry to increase or decrease N* from 0, respectively (Gruber and Sarmiento 1997; Deutsch et al. 2001). Anthropogenic atmospheric nitrogen deposition also produces positive N* values (Kim et al. 2014). However, atmospheric nitrogen deposition is greatest in coastal regions of the western North Pacific Ocean and is not likely a major influence on the food webs of pelagic seabirds that do not frequent coastal waters (Kim et al. 2014). While we cannot dismiss the possibility that atmospheric

nitrogen deposition affects $\delta^{15}N_{Phe}$ gradients, we here consider $\delta^{15}N_{Phe}$ in terms of the relative importance of denitrification and phytoplankton uptake versus nitrogen fixation on nutrient $\delta^{15}N$.

The amino acid $\delta^{15}N$ approach offers an important lens for understanding trophic dynamics of seabirds and the nutrient regimes on which they depend for food. Moreover, chronological records of amino acid $\delta^{15}N$ values provide valuable insight into how food web structure may have shifted over time (Hückstädt et al. 2017; Ostrom et al. 2017; Gagne et al. 2018). The ability of amino acid specific data to expand our understanding of seabird foraging habits and develop a more comprehensive representation of oceanic food webs is facilitated by studying ecologically diverse trans-Pacific predators and carefully selecting tissue types. Whereas the timing of body contour molt is often poorly constrained, remiges more often harbor information related to a specific time period in the annual cycle. For example, the analysis of primary feathers provided unique insights into the non-breeding season foraging habits of the Hawaiian petrel (Wiley et al. 2012; Morra et al. 2018). In contrast to feathers, the slow turnover time of bone collagen offers a record of isotopic information over a period of a year or more. Thus, collagen isotope data spatially integrate dietary information from across the birds' marine distribution, rather than reflecting a single season or foraging location (Rucklidge et al. 1992).

We compared amino acid specific nitrogen isotope data from the Hawaiian petrel to those from two seabirds with distinct foraging strategies—Newell's shearwater and Laysan albatross. Our data from collagen represent year-round foraging habits. The three study species grant extensive spatial coverage of the North Pacific Ocean and exhibit stark ecological contrasts (Fig. 4). Newell's shearwater was once thought to be extinct on the Hawaiian Islands (Mitchell et al. 2005). Unique among our study species, Newell's shearwaters employ pursuit plunging and are capable of catching prey 10 meters beneath the surface (Ainley et al. 1997). Of the study species,

they have the most constrained marine distribution and fly the shortest distance on foraging trips during the breeding season—25% and 33% of Hawaiian petrel and Laysan albatross trip distance, respectively (Fig. 4; Spear et al. 1995; Fernandez et al. 2001; Adams and Flora 2010). In contrast to our other study species, Laysan albatross have a large and stable population (Croxall et al. 2005; BirdLife International 2017) and are not known to feed in association with tuna schools or in mixed-species flocks (Ainley et al. 1997; Simons and Hodges 1998; Awkerman et al. 2009; Ainley et al. 2014). Laysan albatross frequently scavenge, including from fishing vessels whereby they are often killed as bycatch (Cousins et al. 2000), and they are extensively distributed across the North Pacific Ocean (BirdLife International 2017).

In this study, we developed isotope chronologies based on the analysis of $\delta^{15}N_{Phe}$ and $\Delta\delta^{15}N_{Glu\text{-}Phe}$ from bone collagen of Newell's shearwater and Laysan albatross. We used our $\delta^{15}N_{Phe}$ data to assess variation in nutrient regime use and our $\Delta\delta^{15}N_{Glu\text{-}Phe}$ as an indicator of trophic position differences within and among our study species. We compared data extending back as far as a century to published amino acid $\delta^{15}N$ records from the Hawaiian petrel. We also determined the probability that Newell's shearwater and Laysan albatross changed their foraging habits (i.e. the nutrient regime they associate with or their trophic position) during the recent past. In addition to providing insight into seabird foraging dynamics, our study offers a more comprehensive understanding of ecosystem integrity in the North Pacific Ocean over a time when marine ecosystems experienced increased threats.

METHODS

Sample Acquisition

Samples dating from 2001 to present were collected from salvaged carcasses. Acquisition of Hawaiian petrel samples from Haleakalā National Park (Maui) and Hawai'i Volcanoes National Park (Hawai'i) between 2001 and 2010 is described in Wiley et al. (2013). Salvaged Newell's shearwaters predominantly consist of birds found dead after grounding by light attraction or killed by introduced predators. These birds were acquired from Kaua'i between 2013 and 2016 and Laysan albatross from the Hawaii longline fisheries between 2003 and 2014. Samples from prior to 2000 are from museum study skins from collections housed at the National Museum of Natural History, the Bernice Bishop Museum, and the California Academy of Sciences. Samples from after 2000 are designated as the modern time period in each species.

Sample Sizes

Samples from modern and historical specimens were derived from after hatch-year birds. Hawaiian petrels were aged previously by Wiley et al. (2013), and we determined Newell's shearwater ages using the color and shape of primaries (Pyle 2008). For historical Laysan albatross, we referred to the age designation indicated in the museum collection. Modern Laysan albatross were aged based on bursa size; the absence of a bursa indicates the bird was likely greater than 4 years of age (Broughton 1994). We obtained bone samples from 22 Laysan albatross divided evenly between two time periods corresponding to before and after the onset of industrialized fishing in the North Pacific Ocean: pre-1950 (1902-1937; the historical sample) and post-2000 (2003-2014; the modern sample). Of the 11 historical Laysan albatross, 8 were from Laysan Island, the remaining 3 were from Lisianski Island, the Aleutians West Census, and Midway Islands. For Newell's shearwaters, we divided 24 samples into three time periods. The

oldest available museum samples were from 1964-1966 (n = 5); we compared those to two more recent time periods: 9 birds from 1983-1998 and 10 birds from 2013-2016. Newell's shearwaters prior to 2000 originated from Kaua'i (n = 4), Hawai'i (n = 4), Oahu (n = 3), and the North Pacific Ocean within 500 miles of the Hawaiian Islands (n = 3). Ancient and modern Hawaiian petrel data are from Ostrom et al. (2017) and include Maui individuals from the Foundation (1000-1400 CE; 550-950 y B.P., n = 5) and Modern (1950-2010, n = 7) time periods and birds from the island of Hawai'i from the Late Expansion (1400-1800 CE; 150-550 y B.P., n = 8) and Modern (1950-2010, n = 8) time periods. Hawaiian petrel time periods are defined by Kirch (1990) and represent archaeological periods in the development of human societies in the Hawaiian Islands.

Sample Preparation

Collagen was isolated and purified at Michigan State University according to Stafford et al. (1988) as modified by Wiley et al. (2013). Modern and ancient bone fragments (50-200 mg) were scraped with a razor blade and rinsed with ultrapure distilled water (E-pure, Barnstead). Clean bone fragments were demineralized with multiple changes of quartz-distilled 1 N hydrochloric acid. The demineralized samples were soaked in 0.05 N potassium hydroxide overnight to remove humate contaminants and the resulting collagen was lyophilized. Collagen was gelatinized with 0.05 N hydrochloric acid in a 105℃ oven for 1-8 hours and passed through a 0.22 or 0.45 μm Millipore Millex GV filter, then lyophilized again. The resulting gelatin was stored frozen prior to analysis.

Gelatin (0.5-1.2 mg) was hydrolyzed in 0.5 mL of quartz-distilled 12 N hydrochloric acid in a 105℃ oven for approximately 20 hours. Lipids were removed from the resultant filtrate with *n*-hexane/dichloromethane (3:2, v/v), and evaporated to dryness in methanol under a gentle N_2

stream at 50°C. Amino acids in the lipid extracted hydrolysate were esterified and acylated with *N*-pivaloyl/isopropyl (NP/iPr) derivatization (Chikaraishi et al. 2009). Samples were esterified with thionyl chloride/2-propanol (1:4, v/v) at 105°C for 2 hours then acylated with pivaloyl chloride/dichloromethane (1:4, v/v) at 105°C for 2 hours. The amino acid derivatives were extracted with *n*-hexane/dichloromethane (3:2, v/v) and stored at –25°C.

$\delta^{15}N$ Amino Acid Analysis

The nitrogen isotopic composition of individual amino acids was determined by gas chromatography/combustion/isotope ratio mass spectrometry using an Isoprime isotope ratio mass spectrometer (IRMS; Elementar, UK) coupled to a 7890 gas chromatograph (GC; Agilent Technologies, USA) via a combustion and reduction furnace. Combustion and reduction were performed in a glass capillary tube with CuO, NiO, and Pt wires at 950°C. The amino acids were injected on column at 250 °C and separated on a BPX-5 capillary column (60 m x 0.32 mm inner diameter, 1.0 μm film thickness; SGE Analytical Science, USA). The GC oven temperature was programmed as follows: initial temperature 40°C for 2 min, ramp of 10°C min^{-1} to 280°C and hold for 10 min, ramp of 10°C min^{-1} to 325°C and hold for 25 min. Carrier gas (He) flow through the GC column was 1.6 ml min^{-1}. The CO_2 and H_2O generated in the combustion furnace were removed from the sample stream using a liquid nitrogen trap.

Stable isotope values are expressed in per mil (‰) as $\delta^{15}N_a$ = $[(^{15}N/^{14}N_{sample}/^{15}N/^{14}N_{standard})-1] \times 10^3$ relative to the standard, atmospheric N_2. Accuracy was evaluated by daily analysis of external reference mixtures consisting of NP/iPr derivatives of several isotopically characterized amino acids (Gly, Val, Leu, Pro, Asp, Met, Glu, Phe). Reproducibility of the standards was 0.7‰ or better. Samples were analyzed in triplicate with a standard deviation of less than 0.7‰ for Glu and Phe. However, if the reproducibility of Glu and

Phe for duplicates of the same sample was less than or equal to 0.5‰, we reported the average of the two.

Nitrogen isotope analyses for Laysan albatross and Newell's shearwater were conducted at Michigan State University. The analyses for Hawaiian petrel samples from Ostrom et al. (2017) were performed by Yoshito Chikaraishi at the Japan Agency for Marine-Earth Science and Technology using a Delta-plus XP IRMS (Thermo Fisher Scientific) coupled to a 6890 GC (Agilent Technologies) via combustion and reduction furnaces. A blind inter-laboratory comparison on five of our Laysan albatross samples showed no influence of analyst or laboratory. Between laboratories, the average difference in the absolute values of $\delta^{15}N_{Glu}$ and $\delta^{15}N_{Phe}$ was 0.5‰ and 0.3‰, respectively, ensuring the comparability of our three study species.

Model Selection

We evaluated the effect of large scale climatic phenomena (i.e. El Niño Southern Oscillation, ENSO) on Newell's shearwater temporal $\delta^{15}N_{Phe}$ and $\Delta\delta^{15}N_{Glu\text{-}Phe}$ data by including the Multivariate ENSO Index (MEI) and time period (1960's, 1980's-1990's, and post-2000) as independent variables in regression models. $\delta^{15}N_{Phe}$ and $\Delta\delta^{15}N_{Glu\text{-}Phe}$ were evaluated separately. Based on an estimate that avian bone collagen has a half-life of approximately 6 months (Hobson and Clark 1992), we assigned MEI classifications based on the average NOAA MEI ranking for the 18 months prior to the bird's date of death. Model selection was based on Akaike's Information Criterion corrected for finite sample sizes (AICc). The model with the lowest AICc value contained year as the only independent variable, so we did not include MEI in our model.

All historical Laysan albatross samples were from an MEI neutral period, eliminating the need for evaluating the influence of MEI on the historical data. Modern Laysan albatross were

from MEI neutral or moderate La Niña conditions. We asked if $\delta^{15}N_{Phe}$ and $\Delta\delta^{15}N_{Glu\text{-}Phe}$ differed between these two conditions with a two-tailed unpaired t-test that assumed homoscedasticity.

Statistical Analysis

We developed a hierarchical method that accounts for analytical variation and reduces type 1 errors in hypothesis testing. The method consists of two sub-models. The first, the observational model, estimates variation associated with the measurement process using replicate samples. The second, the ecological model, estimates population means and covariance between $\delta^{15}N_{Phe}$ and $\Delta\delta^{15}N_{Glu\text{-}Phe}$ given uncertainty due to analytical error. The observational model is $y[i,j,t,s,1{:}r] \sim mvnorm(\mu_{(i,t,s)}, \sigma)$ and the ecological model is $\mu_{(i,t,s)} \sim mvnorm(M_{(t,s)}, \Sigma_{(t,s)})$ where $y[i,j,t,s,1{:}r]$ is the data vector indexed by individual (i), replicate (j), time bin (t), and species (s), and consisting of isotope values 1:r, where r is the number of amino acid variables used, $\mu_{(i,t,s)}$ is the mean vector of individual i, in time bin t for species s. σ is the covariance matrix (dimensions r by r) associated with the total analytical error shared across all individuals, time bins, and species. $M_{(t)}$ is the population mean vector for time t and species s and $\Sigma_{(t,s)}$, the covariance matrix associated with naturally occurring isotopic variation, was assumed constant within (but not between) time bin t and species s.

The model parameters were estimated in a Bayesian framework using the program JAGS (Plummer 2003) interfaced to R (R Development Core Team 2013). Minimally informative priors were used for estimated parameters (Rossman et al. 2016). The model was fit in JAGS using a Markov Chain Monte Carlo for 100,000 iterations with a 10,000 iteration burn in and three chains. The posterior distributions were thinned at a rate of saving one iteration in every three. Convergence was ensured through monitoring traceplots and Rhat values (Gelman and Hill 2007). The probability that two parameters were different was calculated by summing the

number of posterior estimates in which one parameter was larger than the other dividing by the total number of posterior estimates. Specifically, we report probabilities that $\delta^{15}N_{Phe}$ and $\Delta\delta^{15}N_{Glu\text{-}Phe}$ differ among modern and historical colonies and species, and declined over time.

We also used posterior estimates to visually represent the data and associated uncertainty. Standard ellipses characterize the foraging habits of each population. Estimated population $\delta^{15}N_{Phe}$ and $\Delta\delta^{15}N_{Glu\text{-}Phe}$ means define the center of each standard ellipse and a covariance matrix determines the shape and orientation (Jackson et al. 2011; Rossman et al. 2015). We generated probability density distributions for Newell's shearwater and Laysan albatross $\delta^{15}N_{Phe}$ and $\Delta\delta^{15}N_{Glu\text{-}Phe}$ values, similar to those for the Hawaiian petrel in Ostrom et al. (2017).

RESULTS

Model Selection

In addition to time, we recognize isotope values may be influenced by MEI, however, there was no significant difference in Laysan albatross $\delta^{15}N_{Phe}$ or $\Delta\delta^{15}N_{Glu\text{-}Phe}$ between MEI neutral and moderate La Niña conditions ($\delta^{15}N_{Phe}$ $t = 0.22$, df = 9, $P = 0.83$; $\Delta\delta^{15}N_{Glu\text{-}Phe}$ $t = 0.72$, df = 9, $P = 0.49$). For Newell's shearwaters, the model with the lowest AICc value (39.94, $P = 0.0020$) incorporated year as the only predictor.

Interspecific and Inter-Colony Variation in Amino Acid $\delta^{15}N$

Our results indicate that all three species as well as the Hawaiian petrels breeding on two separate islands likely have significantly different $\Delta\delta^{15}N_{Glu\text{-}Phe}$ means in modern as well as historical time periods ($P \geq 0.99$; Table 6a; Fig. 5), although the historical time period of each species does not reflect the same chronological time. Relative to Newell's shearwaters, Maui Hawaiian petrels likely have a lower $\delta^{15}N_{Phe}$ mean in the historical time period ($P = 0.95$) but not

in the modern time period ($P = 0.70$). In modern and historical time periods, both Hawaiian petrels from Maui and Newell's shearwaters likely have a lower $\delta^{15}N_{Phe}$ mean than Hawaiian petrels from the island of Hawai'i and Laysan albatross ($P \geq 0.95$). There is also high probability that Hawaiian petrels from the island of Hawai'i have a lower $\delta^{15}N_{Phe}$ mean than Laysan albatross in the historical time period ($P = 0.995$).

Temporal Variation in $\delta^{15}N_{Phe}$ and $\Delta\delta^{15}N_{Glu\text{-}Phe}$

The probability that $\delta^{15}N_{Phe}$ declined in Newell's shearwaters over the past 50 years was low (P = 0.27) (Table 6b; Fig. 6). There was a 0.79 probability that $\delta^{15}N_{Phe}$ declined in Laysan albatross over the past 100 years. We did not consider this difference to be ecologically or statistically significant. Our results indicated at least a 0.97 probability that $\Delta\delta^{15}N_{Glu\text{-}Phe}$ declined in Newell's shearwater and Laysan albatross over the past 50 and 100 years, respectively.

DISCUSSION

Modern Time Periods

The two Hawaiian petrel populations occupy unique isotopic niches despite the close proximity of their breeding colonies and their high degree of morphological similarity (Fig 5; Wiley et al. 2012, 2013; Ostrom et al. 2017). The low $\delta^{15}N_{Phe}$ mean of the Maui Hawaiian petrel colony indicates these birds tend to utilize waters characterized by nitrogen fixation that are associated with positive N* (Fig. 5; Ostrom et al. 2017). In contrast, birds from Hawai'i Island likely spend less time foraging in biogeochemical regimes supplied by nitrogen fixation than those from Maui, shown by their higher mean $\delta^{15}N_{Phe}$. Instead, Hawaiian petrels from Hawai'i Island may frequent regions where nutrient sources at the base of the food web are influenced by average

marine nitrate or denitrification and/or substantial phytoplankton uptake. Such regions are characterized by lower N* values than the waters frequented by the Maui population.

The possibility that Hawaiian petrel $\delta^{15}N_{Phe}$ is strongly influenced by differences in nutrient regime is supported by observation and tagging data. Adams and Flora (2010) tracked a breeding adult from Maui making a large counterclockwise loop over the northeast Pacific, which consists of positive and negative N* waters (Fig. 4). During the nonbreeding season, Hawaiian petrels are predominantly distributed south and southeast of Hawaii (Spear et al. 1995; VanZandt 2012), overlapping an area of ^{15}N-enriched water (Altabet and Francois 1994). Differential foraging within a $\delta^{15}N$ gradient could drive inter-colony spatial foraging segregation in Hawaiian petrels.

Interestingly, Hawaiian petrels from Maui appear to occupy a higher trophic position than their Hawai'i Island conspecifics (Fig. 5; Ostrom et al. 2017). This may indicate that food chains supplied by nitrogen fixation are longer than those supplied by nitrate. Multiple factors may contribute to the observed intra-species trophic disparity. Individuals from Maui are slightly larger than those from the Hawai'i colony in some linear dimensions (e.g. culmen and tarsus length, 8% and 10% larger, respectively; Judge et al. 2014) suggesting that Maui Hawaiian petrels are likely capable of consuming larger food items, thereby elevating their trophic position. It is uncertain whether the magnitude of the bill and body size differences between Hawaiian petrel populations is large enough to confer a difference in trophic position. Although body size is often thought to correlate with prey size, some studies find that a 1000-fold range in seabird body mass does not explain diet variation (Ballance et al. 2001). Thus, we considered that Hawaiian petrels from Maui and Hawai'i Islands might specialize on distinct suites of prey

items under the species-level generalist umbrella. Niche partitioning with respect to trophic position and nutrient regime may facilitate population viability.

In addition to intraspecific foraging segregation, we observed isotopic segregation between species. The Newell's shearwater standard ellipse does not overlap with those of the Hawaiian petrel colonies (Fig. 5). The $\delta^{15}N_{Phe}$ mean of Newell's shearwaters is similar to that of Maui Hawaiian petrels, likely resulting from a similar reliance on oceanographic regions characterized by nitrogen fixation. Observational data show that Newell's shearwaters are dispersed across the isotopic gradient extending east from the area of ^{15}N-enriched waters southeast of the Hawaiian Islands (Spear et al. 1995). This could contribute to the population's wide Phe range of 3.7‰. The $\Delta\delta^{15}N_{Glu\text{-}Phe}$ data suggest that Newell's shearwaters occupy a lower trophic position than either of the two Hawaiian petrel populations. Newell's shearwater diet is poorly known. Ainley et al. provided the first report on Newell's shearwater diet in 2014, using stomach contents from carcasses of recently fledged individuals. The diet was dominated by squid (e.g. ommastrephids) with few fish, mainly flying fish. This appears to be similar to Hawaiian petrel diet but with limited data it is unclear how much the relative proportion of diet items differs between species (Spear et al. 1995). If not a result of diet differences, the apparent trophic separation between Hawaiian petrels and Newell's shearwaters may be explained by a difference in body size, given that Newell's shearwaters have a slightly shorter wingspan and lower body mass (Ainley et al. 1997; Simons and Hodges 1998). However, as discussed above, body size differences may not be sufficient to explain the observed divergence in trophic position. The $\Delta\delta^{15}N_{Glu\text{-}Phe}$ differences might also be driven by interactions in mixed-species feeding flocks. Although foraging in large diverse aggregations can improve foraging success, evidence also suggests that intense interference competition can occur, especially among

seabirds employing distinct foraging methods (Schreiber and Burger 2001). For example, surface-seizers, like Hawaiian petrels, might reduce access to prey by diving birds, like Newell's shearwaters, resulting in Newell's shearwaters eating smaller or lower trophic level prey (Schreiber and Burger 2001).

Laysan albatross appear to occupy a distinct niche position. Their $\delta^{15}N_{Phe}$ mean indicates little reliance on food webs supplied by nitrogen fixation (Fig 5). Additionally, Laysan albatross appear to occupy the lowest trophic position of the three species. While our $\Delta\delta^{15}N_{Glu\text{-}Phe}$ data may seem surprising given the large size of this species, recent data from contour feathers and remiges place Laysan albatross at the same or lower trophic position than smaller species (e.g. Bulwer's petrel, *Bulweria bulwerii;* Gagne et al. 2018). While it is difficult to make comparisons between year-round data from collagen and short-term data from feather, data from both tissues emphasize a gap in our knowledge of Laysan albatross trophic dynamics or an unexplored factor controlling $\delta^{15}N$ of amino acids. Diet studies suggest Laysan albatross consume mostly squid, but because they are conducted at colonies or on a specific age class, they provide a limited understanding of diet (Harrison et al. 1983). In addition, stomach content analyses could be compromised by more rapid digestion of soft-bodied organisms that are likely to have a low trophic position (Gould et al. 1997). Such bias would result in an overestimation of their trophic position, a possibility suggested by Gould et al. (1997). Alternatively, we considered whether modern Laysan albatross have low $\Delta\delta^{15}N_{Glu\text{-}Phe}$ because they represent a specific subset of the population (salvaged from fisheries). However, as discussed below, historical Laysan albatross also exhibit low average $\Delta\delta^{15}N_{Glu\text{-}Phe}$, indicating that our results are not simply an attribute associated with one subset of the population. Our data force us to think broadly about the biology of our study species and factors that control $\Delta\delta^{15}N_{Glu\text{-}Phe}$. Diet quality and mode of nitrogen

excretion are two factors that we considered owing to their impact on ^{15}N discrimination and, thus, trophic discrimination factors (McMahon and McCarthy 2016).

If TDF differs acutely among species, inter-specific $\Delta\delta^{15}N_{Glu\text{-}Phe}$ variation may not solely reflect trophic position. This is because trophic position is a function of TDF. The degree of ^{15}N enrichment of Glu between a consumer and its diet, TDF_{Glu}, may be related to diet quality (i.e. amino acid imbalance and protein content; Bradley et al. 2015; Chikaraishi et al. 2015; McMahon et al. 2015; Nielsen et al. 2015; McMahon and McCarthy 2016). If high trophic level organisms have protein rich diets or diets with amino acid compositions similar to their own bodies, they will exhibit low TDF_{Glu}. Thus, if, relative to Hawaiian petrels, Laysan albatross consume a higher quality diet, they could have a lower TDF_{Glu}, which would result in the relatively low $\Delta\delta^{15}N_{Glu\text{-}Phe}$ values we observed. Because our study species are generalist predators with some overlap in the prey they consume, it seems unlikely that differences in TDF account for the $\Delta\delta^{15}N_{Glu\text{-}Phe}$ differences we observe. However, a better understanding of the prey, protein, and amino acid composition of our seabird diets will be important in assessing the influence of diet quality on $\Delta\delta^{15}N_{Glu\text{-}Phe}$.

Alternatively, or in addition to diet composition, metabolic effects might influence our $\Delta\delta^{15}N_{Glu\text{-}Phe}$ data. As a consequence of kinetic isotope effects, the product of a reaction is expected to have a lower isotope value than its substrate. Such isotopic discrimination occurs during nitrogen transformation reactions. Because our study species belong to the same taxonomic order, we do not anticipate large differences in amino acid transformation pathways and associated discrimination against ^{15}N. Instead, differential synthesis of amino acids or loss of excretory nitrogen could produce variation in $\delta^{15}N_{Glu}$, particularly because glutamic acid has a central role in transamination and deamination. In birds, the primary excretory product of

nitrogen metabolism is uric acid. Two of the three nitrogen atoms in uric acid derive from glutamine and, ultimately, glutamic acid, a substrate in glutamine formation. Thus, the loss of ^{14}N during the formation and excretion of uric acid will elevate $\delta^{15}N_{Glu}$. Uric acid can be derived from exogenous or endogenous proteins. But, we do not expect dietary protein to be in excess for the long-ranging seabirds we studied. Production of uric acid from endogenous protein is related to the extent of protein catabolism, and differences in water balance influence uric acid abundance regardless of origin (Jenni and Jenni-Eiermann 1998; Battley et al. 2000; Gerson and Guglielmo 2011; Braun 2015). Catabolism of protein increases under various circumstances such as prolonged flight, breeding, stress, molt, and nutrient limitation, which differ among our study species (Mori and George 1978; Robin et al. 1987, Cherel et al. 1988; Pearcy and Murphy 1997; Jenni and Jenni-Eiermann 1998; Viblanc et al. 2017). Of the three study species, Hawaiian petrels have been observed to fly farthest on a single foraging trip (10,000 km; Spear et al. 1995; Fernández et al. 2001; Adams and Flora 2010). Birds often increase reliance on protein catabolism during extended flights (Gerson and Guglielmo 2011). Laysan albatross often skip a year of breeding whereas Hawaiian petrels and Newell's shearwaters breed annually (Edwards and Rohwer 2005). Moreover, Laysan albatross is the only study species that does not undergo a complete annual primary molt (Edwards and Rohwer 2005). Additionally, our study species exhibit differences in wing loading and flight type (Carey 2012). A plethora of differences among our study species could affect their nitrogen budgets, leading to differential protein catabolism and $\delta^{15}N_{Glu}$ fractionation. However, it is unlikely that the temporal decline in $\Delta\delta^{15}N_{Glu\text{-}Phe}$ observed for all three species was a consequence of identical and simultaneous changes in protein catabolism.

Temporal Variation

Our long-term amino acid $\delta^{15}N$ isotope chronologies reveal that foraging segregation among modern seabird colonies and species is not a recent phenomenon, but has endured over the course of several decades. Moreover, the relative position of each isotopic niche is similar between historical and modern time periods (Fig. 5). $\delta^{15}N_{Phe}$ provides no evidence of a shift in source nitrogen at the base of our study species' food webs. Rather, there is a high probability that, like the Hawaiian petrel (Wiley et al. 2013; Ostrom et al. 2017), Newell's shearwater and Laysan albatross experienced a significant decline in trophic position within the past century. The latter finding is in contrast to the findings of Gagne et al. (2018). This disparity could be related to the fact that Gagne et al. (2018) analyzed feathers that, unlike bone, represent only a short portion of the individual's annual cycle.

Our study species represent two families and diverse foraging strategies, and grant extensive spatial coverage of the world's largest ocean. Our study species also associate with different oceanographic characteristics, such as sea surface temperature and salinity (Schreiber 1984; Spear et al. 1995; Block et al. 2011). The discovery of a trophic decline in three ecologically distinct pelagic predators indicates a remarkably pervasive shift in food web architecture across the North Pacific Ocean. Climate change is a widely accepted driver of oceanic ecosystem change (Cheung et al. 2012; Woodworth-Jefcoats et al. 2013), however, we failed to find an effect of climate on our study species' feeding habits. This is similar to the results of Gagne et al. (2018) for Laysan albatross. Another major anthropogenic force potentially capable of causing a widespread pelagic trophic decline, fishing, likely impacts modern seabird niches. With industrial fisheries, humans have the power to modify vast oceanic ecosystems to a degree once thought impossible. There is mounting evidence that fisheries

compete with marine predators for food and alter distributions as well as abundances of marine organisms (Tasker et al. 2000; Myers and Worm 2003; Ward and Myers 2005; Polovina and Woodworth-Jefcoats 2013).

The amino acid data may signify threats to marine ecosystem integrity, but they also offer important information to seabird conservationists by illuminating at-sea behavior. This is particularly critical for the Hawaiian petrel and Newell's shearwater, which have experienced drastic population declines in recent decades (Raine et al. 2017). The number of Newell's shearwaters nesting on Kaua'i plummeted 94% between 1993 and 2013, largely due to collisions with power lines, light attraction, and predation by introduced predators (Raine et al. 2017). While many of the threats seabirds face on land are well-characterized, seabirds typically spend 90% of their lives at sea (Ballance et al. 2001). Conservation managers cannot assess at-sea risks without sufficient information regarding pelagic distributions and foraging habits. Our results enhance the perspective, brought forth in other studies, that biogeochemical regimes and trophic dynamics of the North Pacific Ocean have recently changed (Wiley et al. 2013; Kim et al. 2014; Sherwood et al. 2014; Ostrom et al. 2017). The emerging challenge is to characterize how a changing oceanographic environment influences population viability, an important consideration given that no species is exempt from the possibility of extinction.

APPENDIX

Figure 4. N* distribution, at-sea distributions of Newell's shearwater, Laysan albatross and Hawaiian petrel, and $\delta^{15}N$ (‰) values of sinking particles and core top sediments. The color gradient is the distribution of N* defined and gridded by Sherwood et al. (2014), where N* = N – 16P + 2.9 µmol $kg^{-}1$, P = phosphorus. Positive N* values are interpreted as an increase in nitrogen fixation and negative values as net denitrification (Sherwood et al. 2014). Curved lines delineate seabird distributions: short dash = Newell's shearwater, long dash = Laysan albatross (north of line), solid = Hawaiian petrel (Ainley et al. 1997; Simons and Hodges 1998; Awkerman et al. 2009). The data for sinking particles and sediments mark an area of elevated $\delta^{15}N$ in the eastern tropical north Pacific Ocean and illustrate an isotopic gradient. As illustrated in Wiley et al. (2012), the isotopic gradient extends in all directions from the area of elevated $\delta^{15}N$. Filled black points represent $\delta^{15}N$ of sinking particles, labeled as follows: a = 8‰, b = 11‰, c = 13‰, d = 8‰; open black points represent $\delta^{15}N$ of core top sediments, labeled as follows: a = 16‰, b = 13‰, c = 11‰, d = 9‰ (Altabet and Francois 1994) The size of filled and open points is positively correlated with the associated $\delta^{15}N$ value.

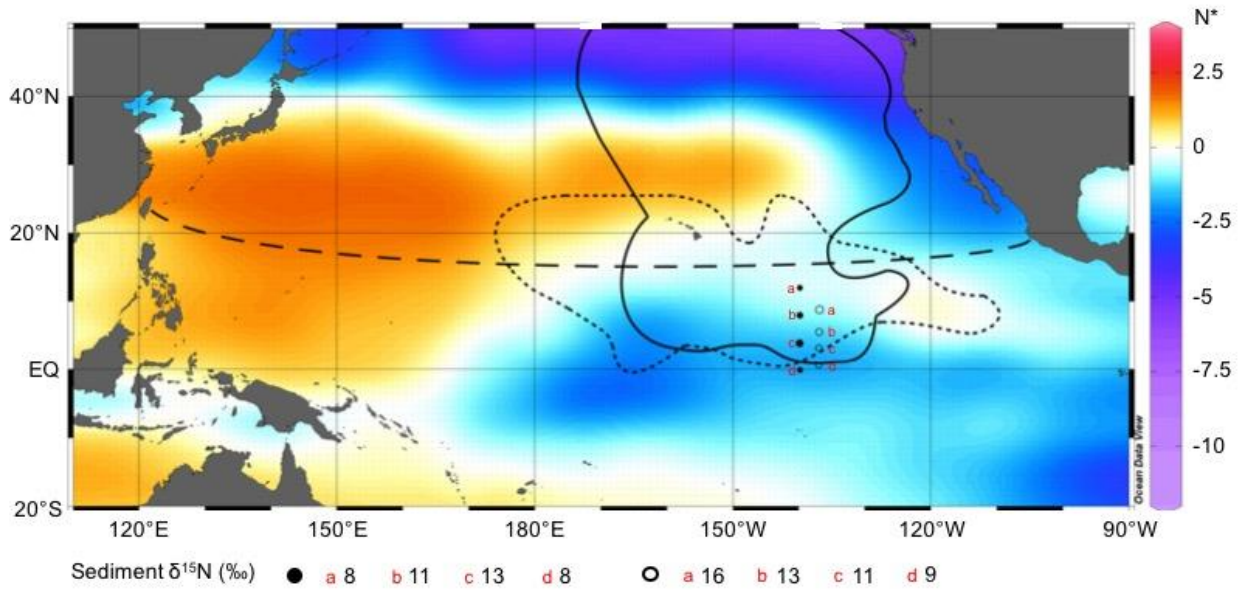

Figure 5. Isotope standard ellipses representing variation in $\delta^{15}N_{Phe}$ and $\Delta\delta^{15}N_{Glu\text{-}Phe}$ (‰) values for (a) historical and (b) modern Newell's shearwater, Laysan albatross and Hawaiian petrel. Model estimated mean $\delta^{15}N_{Phe}$ and $\Delta\delta^{15}N_{Glu\text{-}Phe}$ values for each population define the center of the ellipse and a covariance matrix determines the shape and orientation. Legend indicates species and time period designations. Species abbreviations are as follows: NESH = Newell's shearwater, LAAL = Laysan albatross, HAPE = Hawaiian petrel. Time periods and sample sizes (n) follow. NESH: 1960's (1964-1966, n = 5); 1980's-1990's (1983-1998, n =9); Post-2000 (2013-2016, n = 10); LAAL: Pre-1950 (1902-1937, n = 11); Post-2000 (2003-2014, n = 11); Maui HAPE: Foundation Period (1000-1400 CE; 550-950 y B.P., n = 5); Modern Period (1950-2010, n = 7); Hawai'i HAPE: Late Expansion Period (1400-1800 CE; 150-550 y B.P., n = 8); Modern Period (1950-2010, n = 8). The prehistoric time bins for Maui and Hawai'i correspond with Hawaiian archaeological time periods defined by Kirch (1990).

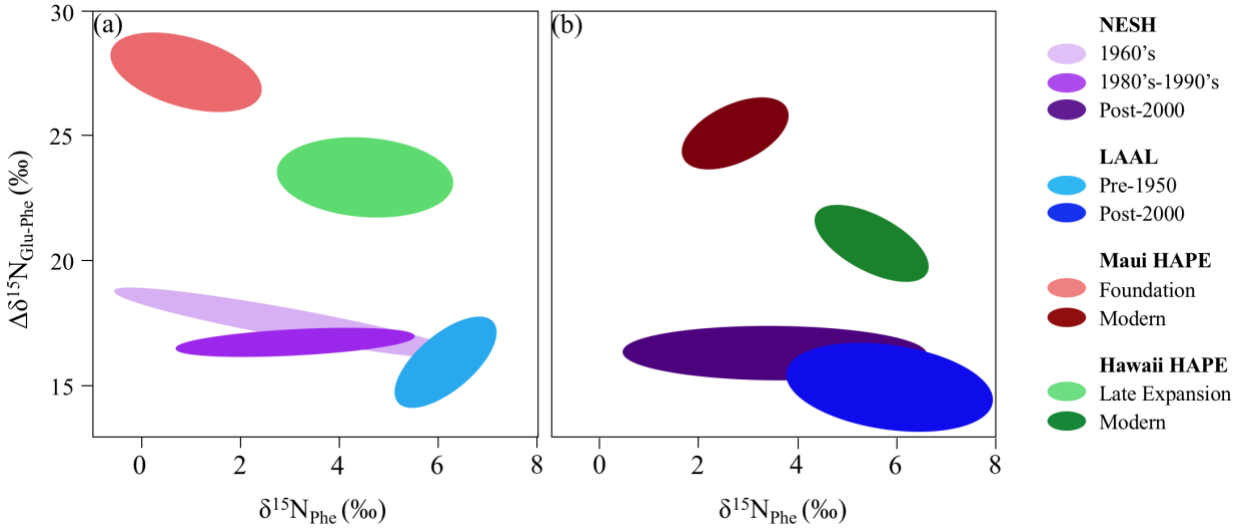

Figure 6. Density distributions of model estimated $\delta^{15}N_{Phe}$ and $\Delta\delta^{15}N_{Glu\text{-}Phe}$ (‰) for (a) Newell's shearwater and (b) Laysan albatross over the past 50 and 100 years, respectively. Newell's Shearwater time periods and sample sizes (n): 1960's (1964-1966, n = 5); 1980's-1990's (1983-1998, n = 9); Post-2000 (2013-2016, n = 10). Laysan albatross time periods and sample sizes: Pre-1950 (1902-1937, n = 11); Post-2000 (2003-2014, n = 11).

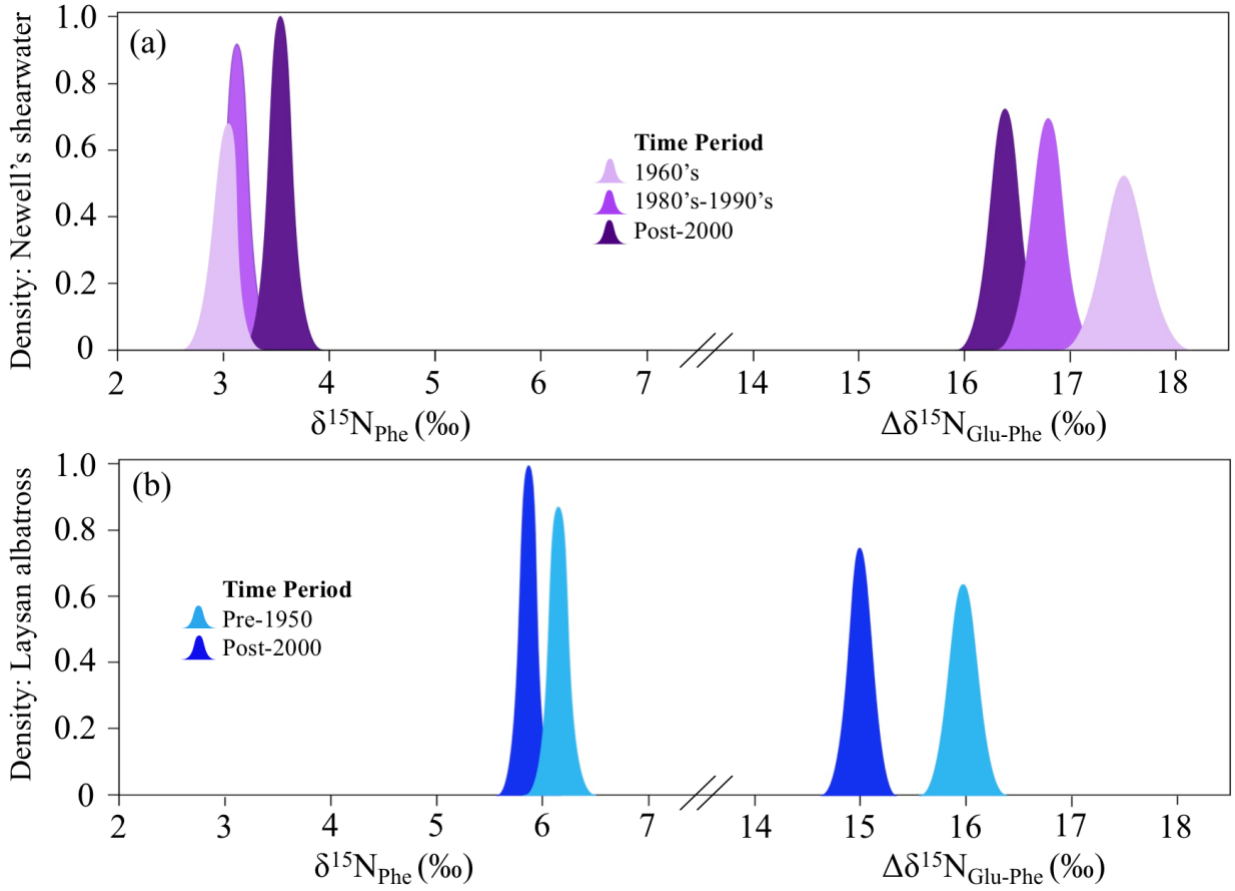

Table 6. Statistical results from hierarchical modeling of collagen isotope data showing variation among groups (colony or species). Probabilities (*P*) indicate likelihood that $\delta^{15}N_{Phe}$ and $\Delta\delta^{15}N_{Glu\text{-}Phe}$ (‰) are greater in group 1 than in group 2. (a) is an inter-population and interspecific comparison of Newell's shearwater (NESH), Laysan albatross (LAAL), and Hawaiian petrel (HAPE) data for historical and modern time periods; (b) is a within species comparison of historical to modern data for NESH and LAAL. Statistical results for comparisons with Maui and Hawai'i HAPE utilize previously published data for HAPE (Ostrom et al. 2017).

(a)

Group 1	Group 2	*P* Group 1 > Group 2 (Modern)		*P* Group 1 > Group 2 (Historical)	
		$\delta^{15}N_{Phe}$ (‰)	$\Delta\delta^{15}N_{Glu\text{-}Phe}$ (‰)	$\delta^{15}N_{Phe}$ (‰)	$\Delta\delta^{15}N_{Glu\text{-}Phe}$ (‰)
Maui HAPE	Hawai'i HAPE	0.0017	1.00	0.0030	1.00
Maui HAPE	NESH	0.30	1.00	0.051	1.00
Maui HAPE	LAAL	0.0005	1.00	0.00018	1.00
Hawai'i HAPE	NESH	1.00	1.00	0.95	1.00
Hawai'i HAPE	LAAL	0.24	1.00	0.0046	1.00
NESH	LAAL	0.000022	1.00	0.0012	0.99

(b)

Group 1 (Historical)	Group 2 (Modern)	*P* Group 1 (Historical) > Group 2 (Modern)	
		$\delta^{15}N_{Phe}$ (‰)	$\Delta\delta^{15}N_{Glu\text{-}Phe}$ (‰)
1960's NESH	1980's-1990's NESH	0.44	0.91
1960's NESH	Post-2000 NESH	0.27	0.97
1980's-1990's NESH	Post-2000 NESH	0.25	0.85
Pre-1950 LAAL	Post-2000 LAAL	0.79	0.98

LITERATURE CITED

LITERATURE CITED

Adams J, Flora S. 2010 Correlating seabird movements with ocean winds: linking satellite telemetry with ocean scatterometry. Mar. Biol. 157: 915-929.

Ainley DG, Telfer TC, Reynolds MH. 1997 Newell's Shearwater (*Puffinus newelli*), version 2.0. In: Rodewald PG (ed) The Birds of North America. Cornell Lab of Ornithology, Ithaca, New York, USA.

Ainley DG, Walker WA, Spencer GC, Holmes ND. 2014 The prey of Newell's shearwater *Puffinus newelli* in Hawaiian waters. Mar. Ornithol. 44: 69-72.

Altabet M, Francois R. 1994 Sedimentary nitrogen isotopic ratio as a recorder for surface ocean nitrate utilization. Glob. Biogeochem. Cycles 8: 103-116.

Awkerman JA, Anderson DJ, Whittow GC. 2009 Laysan Albatross (*Phoebastria immutabilis*), version 2.0. In: Rodewald PG (ed) The Birds of North America. Cornell Lab of Ornithology, Ithaca, New York, USA.

Ballance LT, Pitman RL, Reilly SB. 1997 Seabird community structure along a productivity gradient: importance of competition and energetic constraint. Ecol. 78: 1502-1518.

Ballance LT, Ainley DG, Hunt Jr. GL. 2001 Seabird Foraging Ecology. In: Steele JH, Thorpe SA, Turekian KK (eds) Encyclopedia of Ocean Sciences. Academic Press, London, 5: 2636-2644.

Battley PF, Piersma T, Dietz MW, Tang S, Dekinga A, Hulsman K. 2000 Empirical evidence for differential organ reductions during trans–oceanic bird flight. Proc. R. Soc. B: Biol. Sci. 267: 191-195.

Bearhop S, Phillips RA, McGill R, Cherel Y, Dawson DA, Croxall JP. 2006 Stable isotopes indicate sex-specific and long-term individual foraging specialization in diving seabirds. Mar. Ecol. Prog. Ser. 311: 157-164.

BirdLife International. 2017 IUCN Red List for birds. Downloaded from http://www.birdlife.org on 10/12/2017.

Block BA, Jonsen ID, Jorgensen SJ, Winship AJ, Shaffer SA, Bograd SJ, Hazen EL, Foley DG, Breed GA, Harrison AL, Ganong JE, Swithenbank A, Castleton M, Dewar H, Mate BR, Shillinger GL, Schaefer KM, Benson SR, Weise MJ, Henry RW, Costa DP. 2011 Tracking apex marine predator movements in a dynamic ocean. Nat. 475: 86-90.

Bolnick DI, Svanbäck R, Fordyce JM, Yang LH, Davis JM, Hulsey CD, Forister ML. 2003 The ecology of individuals: incidence and implications of individual specialization. Am. Nat.

161: 1-28.

Bradley CJ, Wallsgrove NJ, Choy CA, Drazen JC, Hetherington ED, Hoen DK, Popp BN. 2015 Trophic position estimates of marine teleosts using amino acid compound specific isotopic analysis. Limnol. Oceanogr: Methods 13: 476-493.

Braun EJ. 2015 Osmoregulatory systems of birds. In: Scanes CG (ed) Sturkie's Avian Physiology, 6th edn. Academic Press, San Diego, California, USA, pp 285-300.

Broughton JM. 1994 Size of the bursa of Fabricius in relation to gonad size and age in Laysan and Black-footed Albatrosses. Condor 96: 203-207.

Carey C. 2012 Avian energetics and nutritional ecology. Springer Science and Business Media, New York, USA.

Casciotti KL, Trull TW, Glover DM, Davies D. 2008 Constraints on nitrogen cycling at the subtropical North Pacific Station ALOHA from isotopic measurements of nitrate and particulate nitrogen. Deep. Res. Part II: Trop. Stud. Oceanogr. 55: 1661-1672.

Cherel Y, Robin JP, Walch O, Karmann H, Netchitailo P, Le Maho Y. 1988 Fasting in king penguin. I. Hormonal and metabolic changes during breeding. Am. J. Physiol.-Regul., Integr. Comp. Physiol., 254: R170-R177.

Cheung WW, Meeuwig JJ, Feng M, Harvey E, Lam VW, Langlois T, Slawinski D, Sun C, Pauly D. 2012 Climate-change induced tropicalisation of marine communities in Western Australia. Mar. Freshw. Res. 63: 415-427.

Chikaraishi Y, Kashiyama Y, Ogawa NO, Kitazato H, Ohkouchi N. 2007 Metabolic control of nitrogen isotope composition of amino acids in macroalgae and gastropods: implications for aquatic food web studies. Mar. Ecol. Prog. Ser. 342: 85-90.

Chikaraishi Y, Ogawa NO, Kashiyama Y, Takano Y, Suga H, Tomitani A, Miyashita H, Kitazato H, Ohkouchi N. 2009 Determination of aquatic food- web structure based on compound-specific nitrogen isotopic composition of amino acids. Limnol. Oceanogr: Methods 7: 740-750.

Chikaraishi Y, Steffan SA, Takano Y, Ohkouchi N. 2015 Diet quality influences isotopic discrimination among amino acids in an aquatic vertebrate. Ecol. Evol. 5: 2048-2059.

Costanza R. 1999 The ecological, economic, and social importance of the oceans. Ecol. Econ. 31: 199-213.

Cousins KL, Dalzell P, Gilman E. 2000 Managing pelagic longline-albatross interactions in the North Pacific Ocean. Mar. Ornithol. 28: 159-174.

Croxall JP, Silk JR, Phillips RA, Afanasyev V, Briggs DR. 2005 Global circumnavigations: tracking year-round ranges of nonbreeding albatrosses. Sci. 307: 249-250.

DeNiro MJ, Epstein S. 1981 Influence of diet on the distribution of nitrogen isotopes in animals. Geochim. Cosmochim. Acta 45: 341-351.

Deutsch C, Gruber N, Key RM, Sarmiento JL, Ganachaud A. 2001 Denitrification and N_2 fixation in the Pacific Ocean. Glob. Biogeochem. Cycles 15: 483-506.

Edwards AE, Rohwer S. 2005 Large-scale patterns of molt activation in the flight feathers of two albatross species. Condor 107: 835-848.

Edwards AE, Fitzgerald SM, Parrish JK, Klavitter JL, Romano MD. 2015 Foraging strategies of Laysan albatross inferred from stable isotopes: implications for association with fisheries. PLoS One 10: e0133471.

Fernández P, Anderson DJ, Sievert PR, Huyvaert KP. 2001 Foraging destinations of three low-latitude albatross (Phoebastria) species. J. of Zool. 254: 391-404.

Gaebler OH, Choitz HC, Vitti TG, Vukmirovich R. 1963 Significance of N^{15} excess in nitrogenous compounds of biological origin. Can. J. of Biochem. and Physiol. 41: 1089-1097.

Gagne TO, Hyrenbach KD, Hagemann ME, Van Houtan KS. 2018 Trophic signatures of seabirds suggest shifts in oceanic ecosystems. Sci. Adv. 4: eaao3946.

Gelman A, Hill J. 2007 Data analysis using regression and multilevel/hierarchical models. Cambridge University Press, New York, USA.

Gerson AR, Guglielmo CG. 2011 Flight at low ambient humidity increases protein catabolism in migratory birds. Sci. 333: 1434-1436.

Gould P, Walker W, Ostrom P. 1997 Foods of northern fulmars associated with high-seas drift nets in the transitional region of the North Pacific. Northwest. Nat. 78: 57-61.

Graham BS, Koch PL, Newsome SD, McMahon KW, Aurioles D. 2010 Using isoscapes to trace the movements and foraging behavior of top predators in oceanic ecosystems. In: West JB, Bowen GJ, Dawson TE, Tu KP (eds) Isoscapes: Understanding Movement, Pattern, and Process on Earth Through Isotope Mapping. Springer Science, Dordrecht, The Netherlands, pp 299-318.

Gruber N, Sarmiento JL. 1997 Global patterns of marine nitrogen fixation and denitrification. Glob. Biogeochem. Cycles 11: 235-266.

Hinke JT, Polito MJ, Goebel ME, Jarvis S, Reiss CS, Thorrold SR, Trivelpiece WZ, Watters GM. 2015 Spatial and isotopic niche partitioning during winter in chinstrap and Adélie penguins from the South Shetland Islands. Ecosphere 6: 125.

Hobson KA, Clark RG. 1992 Assessing avian diets using stable isotopes I: Turnover of ^{13}C in tissues. Condor 94: 181-188.

Hückstädt LA, McCarthy MD, Koch PL, Costa DP. 2017 What difference does a century make? Shifts in the ecosystem structure of the Ross Sea, Antarctica, as evidenced from a sentinel species, the Weddell seal. Proc. R. Soc. B 284: 20170927.

Jackson AL, Inger R, Parnell AC, Bearhop S. 2011 Comparing isotopic niche widths among and within communities: SIBER—Stable Isotope Bayesian Ellipses in R. J. Anim. Ecol. 80: 595-602.

Karl D, Letelier R, Tupas L, Dore J, Christian J, Hebel D. 1997 The role of nitrogen fixation in biogeochemical cycling in the subtropical North Pacific Ocean. Nat. 388: 533-538.

Kim IN, Lee K, Gruber N, Karl DM, Bullister JL, Yang S, Kim TW. 2014 Increasing anthropogenic nitrogen in the North Pacific Ocean. Sci. 346: 1102-1106.

Kirch PV. 1990 The evolution of sociopolitical complexity in prehistoric Hawaii: An assessment of the archaeological evidence. J. World. Prehist. 4: 311-345.

Jenni L, Jenni-Eiermann S. 1998 Fuel supply and metabolic constraints in migrating birds. J. Avian Biol. 29: 521-528.

Judge SW, Hu D, Bailey CN. 2014 Comparative analyses of Hawaiian Petrel *Pterodroma sandwichensis* morphometrics. Mar. Ornithol. 42: 81-84.

McClelland JW, Montoya JP. 2002 Trophic relationships and the nitrogen isotopic composition of amino acids in plankton. Ecol. 83: 2173-2180.

McMahon KW, Thorrold SR, Elsdon TS, Mccarthy MD. 2015 Trophic discrimination of nitrogen stable isotopes in amino acids varies with diet quality in a marine fish. Limnol. Oceanogr. 60: 1076-1087.

McMahon KW, McCarthy, MD. 2016 Embracing variability in amino acid $\delta^{15}N$ fractionation: mechanisms, implications, and applications for trophic ecology. Ecosphere 7: e01511.

Minagawa M, Wada E. 1984 Stepwise enrichment of ^{15}N along food chains: further evidence and the relation between $\delta^{15}N$ and animal age. Geochim. Cosmochim. Acta 48: 1135-1140.

Mitchell C, Ogura C, Meadows DW, Kane A, Strommer L, Fretz S, Leonard D, McClung A. 2005 Hawaii's comprehensive wildlife conservation strategy. Department of Land and Natural Resources, Honolulu, Hawaii, USA.

Mori JG, George JC. 1978 Seasonal changes in serum levels of certain metabolites, uric acid and calcium in the migratory Canada goose (Branta canadensis interior). Comp. Biochem. Physiol. Part B: Comp. Biochem. 59: 263-269.

Morra KE, Wiley AE, James HF, Dutcher A, Ostrom PH. 2018 Influence of feather selection and sampling protocol on interpretations of Hawaiian Petrel (*Pterodroma sandwichensis*) nonbreeding season foraging habits from stable isotope analysis. Waterbirds 41: 93-100.

Myers RA, Worm B. 2003 Rapid worldwide depletion of predatory fish communities. Nat. 423: 280-283.

Nielsen JM, Popp BN, Winder M. 2015 Meta-analysis of amino acid stable nitrogen isotope ratios for estimating trophic position in marine organisms. Oecologia 178: 631-642.

Ohkouchi N, Chikaraishi Y, Close HG, Fry B, Larsen T, Madigan DJ, McCarthy MD, McMahon KW, Nagata T, Naito YI, Ogawa NO, Popp BN, Steffan S, Takano Y, Tayasu I, Wyatt ASJ, Yamaguchi YT, Yokoyama Y. 2017 Advances in the application of amino acid nitrogen isotopic analysis in ecological and biogeochemical studies. Org. Geochem. 113: 150-174.

Ostrom PH, Wiley AE, James HF, Rossman S, Walker WA, Zipkin EF, Chikaraishi Y. 2017 Broad-scale trophic shift in the pelagic North Pacific revealed by an oceanic seabird. Proc. R. Soc. B 284: 20162436-20162442.

Pearcy SD, Murphy ME. 1997 Essential amino acid metabolism in molting and non-molting sparrows in different nutritional states. Comp. Biochem. Physiol. Part A: Physiol. 118: 1157-1163.

Plummer M. 2003 JAGS: a program for analysis of Bayesian graphical models using Gibbs Sampling. Proceedings of the Third International Workshop on Distributed Statistical Computing. R Project for Statistical Computing, Vienna, Austria.

Polovina JJ, Woodworth-Jefcoats PA. 2013 Fishery-induced changes in the subtropical Pacific pelagic ecosystem size structure: observations and theory. PLoS One 8: e62341.

Pyle P. 2008 Molt and age determination in Procellariiformes. In: Identification Guide to North American Birds, Part 2. Slate Creek Press, Point Reyes Station, CA, USA, pp 248-260.

R Development Core Team. 2013 R: a language and environment for statistical computing. R Foundation for Statistical Computing, Vienna, Austria.

Raine AF, Holmes ND, Travers M, Cooper BA, Day RH. 2017 Declining population trends of Hawaiian Petrel and Newell's Shearwater on the island of Kaua'i, Hawaii, USA. Condor 119: 405-415.

Robin JP, Cherel Y, Girard H, Géloen A, Le Maho Y. 1987 Uric acid and urea in relation to protein catabolism in long-term fasting geese. J. Comp. Physiol. B 157: 491-499.

Rossman S, Ostrom PH, Stolen M, Barros NB, Gandhi H, Stricker CA, Wells RS. 2015 Individual specialization in the foraging habits of female bottlenose dolphins living in a trophically diverse and habitat rich estuary. Oecologia 178: 415-425.

Rossman S, Ostrom PH, Gordon F, Zipkin EF. 2016 Beyond carbon and nitrogen: guidelines for estimating three-dimensional isotopic niche space. Ecol. and Evol. 6: 2405-2413.

Rucklidge GJ, Milne G, McGaw BA, Milne E, Robins SP. 1992 Turnover rates of different collagen types measured by isotope ratio mass spectrometry. Biochim. Biophys. Acta 1156: 57-61.

Schreiber RW. 1984 Tropical seabird biology. Cooper Ornithological Society, Kansas, USA.

Schreiber EA, Burger J. 2001 Biology of marine birds. CRC Press, Florida, USA.

Sherwood OA, Guilderson TP, Batista FC, Schiff JT, McCarthy MD. 2014 Increasing subtropical North Pacific Ocean nitrogen fixation since the Little Ice Age. Nat. 505: 78-81.

Sigman DM, Mccorkle DC, Francois R, Fischer G. 2000 The $\delta^{15}N$ of nitrate in the Southern Ocean: nitrogen cycling and circulation in the ocean interior. J. Geophys. Res. 105: 19599-19614.

Simons TR, Hodges CN. 1998 Hawaiian Petrel (*Pterodroma sandwichensis*), version 2.0. In: Rodewald PG (ed) The Birds of North America. Cornell Lab of Ornithology, Ithaca, New York, USA.

Spear LB, Ainley DG, Nur N, Howell SNG. 1995 Population size and factors affecting at-sea distributions of four endangered Procellariids in the tropical Pacific. Condor 97: 613-638.

Stafford TW, Brendel K, Duhamel RC. 1988 Radiocarbon, ^{13}C and ^{15}N analysis of fossil bone: Removal of humates with XAD-2 resin. Geochim. Chosmochim. Acta 52: 2257-2267.

Tasker ML, Camphuysen CJ, Cooper J, Garthe S, Montevecchi WA, Blaber SJ. 2000 The impacts of fishing on marine birds. ICES J. Mar. Sci. 57: 531-547.

VanZandt ML. 2012 Distribution and habitat selection of the endangered Hawaiian Petrel (*Pterodroma sandwichensis*), from the island of Lāna'i. PhD dissertation, University of Hawaii at Hilo, Hawaii, USA.

Viblanc VA, Schull Q, Cornioley T, Stier A, Ménard JJ, Groscolas R, Robin JP. in press An integrative appraisal of the hormonal and metabolic changes induced by acute stress using king penguins as a model. Gen. Comp. Endocrinol.

Ward P, Myers RA. 2005 Shifts in open-ocean fish communities coinciding with the commencement of commercial fishing. Ecol. 86: 835-847.

Wiley AE, Welch AJ, Ostrom PH, James HF, Stricker CA, Fleischer RC, Gandhi H, Adams J, Ainley DG, Duvall F, Holmes N. 2012 Foraging segregation and genetic divergence between geographically proximate colonies of a highly mobile seabird. Oecologia 168: 119-130.

Wiley AE, Ostrom PH, Welch AJ, Fleischer RC, Gandhi H, Southon JR, Stafford Jr. TR, Penniman JR, Hu D, Duvall FP, James HF. 2013 Millennial-scale isotope records from a wide-ranging predator show evidence of recent human impact to oceanic food webs. Proc. Natl. Acad. Sci. 110: 8972-8977.

Woodworth-Jefcoats PA, Polovina JJ, Dunne JP, Blanchard JL. 2013 Ecosystem size structure response to 21st century climate projection: large fish abundance decreases in the central North Pacific and increases in the California Current. Glob. Chang. Biol. 19: 724-733.

CHAPTER 3

Seasonal Variation in Foraging Habits of Two Hawaiian Seabirds

ABSTRACT

Pelagic seabirds confront many challenges as they course vast expanses of the open ocean in search of food. We evaluated seasonal differences in foraging habits of two ecologically distinct species, Newell's shearwater and Laysan albatross, and for Laysan albatross, extended this seasonal analysis back 100 years. Our assessment of foraging habits relied on amino acid $\delta^{15}N$ proxies for nutrient regime use ($\delta^{15}N_{Phe}$) and trophic position ($\Delta\delta^{15}N_{Glu\text{-}Phe}$). Seasonal differences were revealed by contrasting data from feather grown during the nonbreeding season and data from collagen, which incorporates an average of foraging habits over a year or more. Our results show that Newell's shearwater and Laysan albatross foraging habits differ between breeding and nonbreeding seasons. Despite the fact that both species breed on the Hawaiian Islands, they use different foraging strategies depending on the season. While the nonbreeding season foraging habits of Laysan albatross have persisted over the past century, the seabirds experienced a trophic decline that was exclusive to the breeding season. In addition to addressing threats on land, conservation management strategies for threatened seabirds, including Newell's shearwater and Laysan albatross, will require an understanding of at-sea risks on seasonal timescales and may need to be tailored for individual species.

INTRODUCTION

About 90% of a pelagic seabird's life is spent over the open ocean. Here, they contend with spatially and temporally variable oceanographic conditions, often while navigating thousands of kilometers in search of food (Ballance et al. 2001). The foraging strategies seabirds employ to overcome the challenges of a pelagic lifestyle are difficult to characterize. Pelagic seabirds are inaccessible for most of their lives. They feed far from land, they remain entirely at sea during the nonbreeding season and, in many cases, during the first several years of life, as well (Ballance et al. 2006). The importance of investigating at-sea behavior is recognized, particularly in the context of recent oceanographic change (Lewison et al. 2012; Wiley et al. 2013; Ostrom et al. 2017; Gagne et al. 2018). However, our understanding of how flexible seabird foraging strategies are in response to oceanographic changes within a single year and over several decades is incomplete. Such flexibility could include shifts in feeding location or dietary characteristics, like trophic position. Without an understanding of both breeding and nonbreeding season foraging, it is unclear whether oceanographic changes differentially affect seabirds over the course of the annual cycle.

Studies of pelagic seabird foraging ecology have relied on stomach contents, satellite tagging and stable isotope analysis (Cherel 2008; Cook et al. 2013; Conners et al. 2015). Diet and satellite tagging involve handling live birds—sometimes repeatedly. Such approaches may not be desirable, especially for endangered or threatened species. Yet, tagging studies can offer insights into feeding locations and strategies if parameters like flight speed, turning rates, and area-restricted-searching are monitored (Adams and Flora 2010). While stomach content analyses provide information on prey ingested, they are influenced by differential digestion, reflect only short-term diet, and are often conducted on a specific subset of the population that

can be easily accessed, such as chicks or adults on breeding grounds (Harrison et al. 1983; Ainley et al. 2014). The analysis of carbon and nitrogen isotopes values offers information on trophic level and foraging location (Cherel 2008; Wiley et al. 2013;). Because these analyses may be performed on the tissues of salvaged birds or museum specimens, they do not compromise live animals and reveal unique information complementary to stomach content analyses and tagging studies.

There are numerous examples of the application of nitrogen isotope analysis in seabird foraging ecology, particularly for the identification of trophic level (Farmer and Leonard 2011; Jaeger et al. 2013; Edwards et al. 2015; Hinke et al. 2015). These studies rely on the observation that whole tissue $\delta^{15}N$ systematically increases ~3-4 ‰ with each trophic transfer (Minagawa and Wada; Young et al. 2010). Several studies have taken advantage of the fact that different tissues record foraging information over discrete time periods determined by the tissue's turnover time (Young et al. 2010; Wiley et al. 2012). For example, bone collagen incorporates an average of foraging habits over a year or more, while feathers reflect foraging during their growth, on the scale of days to weeks (Rucklidge et al. 1992; Wiley et al. 2010). Regardless of tissue type, whole tissue $\delta^{15}N$ values can be challenging to interpret because they are influenced by source nitrogen at the base of the food web as well as an organism's trophic position. However, compound specific nitrogen isotope analysis can separate these source and trophic effects (McClelland and Montoya 2002; McCarthy et al. 2007; Chikaraishi et al. 2007; Popp et al. 2007; Ohkouchi et al. 2017). The $\delta^{15}N$ of "source" amino acids, such as phenylalanine ($\delta^{15}N_{Phe}$), undergoes minimal fractionation during trophic transfer, remaining faithful to the isotope value of source nitrogen (e.g. nitrate, ammonium) at the base of the food web. As such, $\delta^{15}N_{Phe}$ can be used as a nutrient proxy. In contrast, the $\delta^{15}N$ of "trophic" amino acids, such as

glutamic acid ($\delta^{15}N_{Glu}$), becomes ^{15}N-enriched with increasing trophic level. This ^{15}N enrichment occurs during metabolic reactions (such as deamination) that discriminate against ^{15}N. The difference between the $\delta^{15}N$ of Glu and Phe functions as a trophic proxy ($\Delta\delta^{15}N_{Glu\text{-}Phe}$) and is used to calculate trophic position (TP): $TP = (\delta^{15}N_{Glu} - \delta^{15}N_{Phe} - \beta)/TDF + 1$, where β is the difference between $\delta^{15}N_{Glu}$ and $\delta^{15}N_{Phe}$ in primary producers and TDF is the trophic discrimination factor, or the net elevation between $\delta^{15}N_{Glu}$ and $\delta^{15}N_{Phe}$ per trophic step (McMahon and McCarthy 2016). Because of the similarity in TDF between feather and bird muscle, and muscle and collagen, the $\Delta\delta^{15}N_{Glu\text{-}Phe}$ of feather and collagen are comparable (Chikaraishi et al. 2014; Hebert et al. 2016; McMahon and McCarthy 2016; Blanke et al. 2017). As a consequence, we can evaluate seasonal differences in trophic dynamics using flight feathers molted post-breeding and collagen that is assimilated year-round.

$\delta^{15}N_{Phe}$ lends itself to the study of seabird foraging ecology because the $\delta^{15}N$ of source nitrogen varies with biogeochemical processes across the Pacific Ocean. The primary nitrogen source that supplies oceanic food webs is nitrate, which has a $\delta^{15}N$ of 5-6 ‰ (Altabet and Francois 1994). While denitrification and phytoplankton uptake elevate the $\delta^{15}N$ of nutrients, food webs influenced by nitrogen fixation—for example, waters near the Hawaiian Islands—have lower values than those supplied by average marine nitrate (Karl et al. 1997; Sigman et al. 2000; Casciotti et al. 2008). Spatial variation in these different nutrient regimes produces isotopic gradients within the north Pacific Ocean (Altabet and Francois 1994; Graham et al. 2010). One such gradient located southeast of the Hawaiian Islands with a conspicuous localized region of ^{15}N-enriched waters around 4-10 °N and 135-140 °W. Because $\delta^{15}N_{Phe}$ values of consumers reflect the $\delta^{15}N$ of source nitrogen, they reveal the biogeochemical regimes on which seabirds depend for food.

$\Delta\delta^{15}N_{Glu\text{-}Phe}$ and $\delta^{15}N_{Phe}$ of feathers can resolve seasonal foraging habits when the timing and sequence of molt is known. Relative to body contours, the molt of remiges is often better constrained (Warham 1996). For example, remiges can provide foraging information related to a specific stage of the annual cycle (Warham 1996). As Procellariiformes, our study species—Newell's shearwater (*Puffinus newelli)* and Laysan albatross (*Phoebastria immutabilis*)—molt their ten primaries during the nonbreeding season (Warham 1996; Edwards and Rohwer 2005). Primary molt in Newell's shearwaters takes place annually. As with other shearwaters, it likely begins at the innermost primary (P1) and proceeds distally (Warham 1996). Laysan albatross flight feather molt is complicated with one of four molt patterns—classified as large, medium, or small in scope—occurring annually (Edwards and Rohwer 2005). Only the outer three primaries are necessarily molted every year and of these, primary 10 (P10) is always molted last (Langston and Rohwer 1996). Isotope analysis of primary feathers that are replaced annually near the end of the nonbreeding season will paint the best picture of post-breeding foraging habits, when the birds are not tied to the colony. Thus, for Newell's shearwater, we analyzed primary 9 (P9); for Laysan albatross, we selected P10 for analysis.

In this study, we compare modern nonbreeding season to year-round foraging habits using $\Delta\delta^{15}N_{Glu\text{-}Phe}$ and $\delta^{15}N_{Phe}$ of primary feathers and bone collagen, respectively, for two ecologically distinct species—Newell's shearwater and Laysan albatross. Given that isotopic differences between feather and collagen must derive from the breeding season, we can draw inferences about breeding season foraging. Additionally, we evaluate Laysan albatross seasonal foraging habits over the past century to determine whether the trophic decline occurred and if it was associated with a particular stage of the annual cycle.

METHODS

Sample Acquisition

Samples dating from 2003 to present were collected from salvaged carcasses and are designated as the modern time period in each species. Salvaged Newell's shearwaters were acquired from Kaua'i between 2013 and 2016 and primarily consist of birds found dead after grounded by light attraction or killed by introduced predators. Salvaged Laysan albatross were collected from the Hawaii longline fisheries between 2003 and 2014. Laysan albatross samples from prior to 1950 make up the historical time period. These samples are from museum study skins from collections housed at the National Museum of Natural History and the California Academy of Sciences.

Sample Sizes

Samples from all specimens were derived from after hatch-year birds. We determined Newell's shearwater ages using the color and shape of primaries (Pyle 2008). For historical Laysan albatross, we referred to the age designation indicated in the museum collection. Modern Laysan albatross were aged based on bursa size; the absence of a bursa indicates the bird was at least four years old and likely of breeding age (Broughton 1994). Newell's shearwater samples were taken from the base of primary 9 (n=10); Laysan albatross samples were from the base of primary 10 (n=19). Laysan albatross samples were divided between two time periods corresponding to before and after the onset of industrialized fishing in the North Pacific Ocean: historical (1902-1937, n=9) and modern (2003-2014, n=10). Of the historical samples, 6 individuals were from Laysan Island and the remaining 3 were from Lisianski Island, the Aleutians West Census, and Midway Islands. For both study species, bone collagen from the same individuals was previously extracted and prepared as described in Chapter 2.

Sample Preparation

Barbs (~0.5mg) were plucked from the base of the feather with forceps, washed (87:13 v/v chloroform:methanol), rinsed with ultrapure distilled water (E-Pure, Barnstead), and dried (25°C). Cleaned feather barbs were cut into thirds and hydrolyzed in 0.5 mL of quartz-distilled 12 N hydrochloric acid in a 105°C oven for approximately 20 hours. Lipids were removed from the resultant filtrate with *n*-hexane/dichloromethane (3:2, v/v), and evaporated to dryness in methanol under a gentle N_2 stream at 50°C. Amino acids in the lipid extracted hydrolysate were esterified and acylated with *N*-pivaloyl/isopropyl (NP/iPr) derivatization (Chikaraishi et al. 2009). Samples were esterified with thionyl chloride/2-propanol (1:4, v/v) at 105°C for 2 hours then acylated with pivaloyl chloride/dichloromethane (1:4, v/v) at 105°C for 2 hours. The amino acid derivatives were extracted with *n*-hexane/dichloromethane (3:2, v/v) and stored at -25°C.

$\delta^{15}N$ Amino Acid Analysis

The nitrogen isotopic composition of individual amino acids was determined by gas chromatography/combustion/isotope ratio mass spectrometry using an Isoprime isotope ratio mass spectrometer (IRMS; Elementar, UK) coupled to a 7890 gas chromatograph (GC; Agilent Technologies, USA) via a combustion and reduction furnace. Combustion and reduction were performed in a glass capillary tube with CuO, NiO, and Pt wires at 950°C. The amino acids were injected on column at 250 °C and separated on a BPX-5 capillary column (60 m x 0.32 mm inner diameter, 1.0 μm film thickness; SGE Analytical Science, USA). The GC oven temperature was programmed as follows: initial temperature 40°C for 2 min, ramp of 10°C min^{-1} to 280°C and hold for 10 min, ramp of 10°C min^{-1} to 325°C and hold for 25 min. Carrier gas (He) flow through the GC column was 1.6 ml min^{-1}. The CO_2 and H_2O generated in the combustion furnace was removed from the sample stream using a liquid nitrogen trap.

Stable isotope values are expressed in per mil (‰) as $\delta^{15}N_a$ = $[(^{15}N/^{14}N_{sample}/^{15}N/^{14}N_{standard}) - 1] \times 10^3$ relative to the standard, atmospheric N_2. Accuracy was evaluated by daily analysis of external standard mixtures consisting of NP/iPr derivatives of several isotopically characterized amino acids (Gly, Val, Leu, Pro, Asp, Met, Glu, Phe). Reproducibility of the standards was 0.7‰ or better. Samples were analyzed in triplicate with a standard deviation of less than 0.7‰ for Glu and Phe. However, if the reproducibility of Glu and Phe for duplicates of the same sample was less than or equal to 0.5‰, we reported the average of the two.

Model Selection

We considered the effect of large scale climatic phenomena (i.e. El Niño Southern Oscillation, ENSO) on our temporal $\delta^{15}N_{Phe}$ and $\Delta\delta^{15}N_{Glu\text{-}Phe}$ data. All historical Laysan albatross samples were from an MEI neutral period, eliminating the need for evaluating the influence of MEI on these data. Modern Laysan albatross samples were from MEI neutral (n=7) or moderate La Niña (n=3) conditions. Most of our Newell's shearwater samples were from MEI neutral conditions (n=8), with only 2 from moderate El Niño conditions. Within each species, we asked if $\delta^{15}N_{Phe}$ and $\Delta\delta^{15}N_{Glu\text{-}Phe}$ differed between MEI conditions with a two-tailed unpaired t-test that assumed homoscedasticity.

Statistical Analysis

We developed a hierarchical method that accounts for analytical variation and reduces type 1 errors in hypothesis testing. The method consists of two sub-models. The first, the observational model, estimates variation associated with the measurement process using replicate samples. The second, the ecological model, estimates population means and covariance between $\delta^{15}N_{Phe}$ and $\Delta\delta^{15}N_{Glu\text{-}Phe}$ given uncertainty due to analytical error. The observational model is

$y[i,j,t,s,1{:}r] \sim mvnorm(\mu_{(i,t,s)}, \sigma)$ and the ecological model is $\mu_{(i,t,s)} \sim mvnorm(M_{(t,s)}, \Sigma_{(t,s)})$ where $y[i,j,t,s,1{:}r]$ is the data vector indexed by individual (i), replicate (j), time bin (t), and species (s), and consisting of isotope values 1:r, where r is the number of amino acid isotope variables used, $\mu_{(i,t,s)}$ is the mean vector of individual i, in time bin t for species s. σ is the covariance matrix (dimensions r by r) associated with the total analytical error shared across all individuals, time bins, and species. $M_{(t)}$ is the population mean vector for time t and species s and $\Sigma_{(t,s)}$, the covariance matrix associated with naturally occurring isotopic variation, was assumed constant within (but not between) time bin t and species s.

The model parameters were estimated in a Bayesian framework using the program JAGS (Plummer 2003) interfaced to R (R Development Core Team 2013). Minimally informative priors were used for estimated parameters (Rossman et al. 2016). The model was fit in JAGS using a Markov Chain Monte Carlo for 100,000 iterations with a 10,000 iteration burn in and three chains. The posterior distributions were thinned at a rate of saving one iteration in every three. Convergence was ensured through monitoring traceplots and Rhat values (Gelman and Hill 2007). The probability that two parameters were different was calculated by summing the number of posterior estimates in which one parameter was larger than the other and dividing by the total number of posterior estimates. Specifically, we report probabilities that $\delta^{15}N_{Phe}$ and $\Delta\delta^{15}N_{Glu\text{-}Phe}$ differ between tissue types and between species, and for Laysan albatross, that they declined over time.

We also used posterior estimates of $\delta^{15}N_{Phe}$ and $\Delta\delta^{15}N_{Glu\text{-}Phe}$ to develop standard ellipses and probability density distributions. Estimated population $\delta^{15}N_{Phe}$ and $\Delta\delta^{15}N_{Glu\text{-}Phe}$ means define the center of each standard ellipse and a covariance matrix determines the shape and orientation

(Jackson et al. 2011; Rossman et al. 2015). Standard ellipses characterize the foraging habits of modern Newell's shearwater and Laysan albatross by tissue type. The probability density distributions were generated for modern and historical Laysan albatross feather and collagen $\delta^{15}N_{Phe}$ and $\Delta\delta^{15}N_{Glu\text{-}Phe}$ values.

RESULTS

Climate Effects

There was no significant difference in Laysan albatross $\delta^{15}N_{Phe}$ or $\Delta\delta^{15}N_{Glu\text{-}Phe}$ between MEI neutral and moderate La Niña conditions ($\delta^{15}N_{Phe}$ t = 1.9, df = 8, P = 0.10; $\Delta\delta^{15}N_{Glu\text{-}Phe}$ t = 1.4, df = 8, P = 0.19). For Newell's shearwaters, there was no difference in $\delta^{15}N_{Phe}$ or $\Delta\delta^{15}N_{Glu\text{-}Phe}$ between MEI neutral and moderate El Niño conditions ($\delta^{15}N_{Phe}$ t = 0.13, df = 8, P = 0.90; $\Delta\delta^{15}N_{Glu\text{-}Phe}$ t = 2.1, df = 8, P = 0.06).

Variation in $\delta^{15}N_{Phe}$ and $\Delta\delta^{15}N_{Glu\text{-}Phe}$ Between Feather and Bone Collagen

Our results indicate that modern Newell's shearwaters had higher $\delta^{15}N_{Phe}$ and lower $\Delta\delta^{15}N_{Glu\text{-}Phe}$ means in feather relative to bone collagen (Table 7a, P > 99%; Fig. 7). Modern Laysan albatross had lower $\delta^{15}N_{Phe}$ and higher $\Delta\delta^{15}N_{Glu\text{-}Phe}$ means in feather relative to bone collagen (Table 7a, $P \geq$ 99%; Fig. 7). Historically, Laysan albatross feather $\delta^{15}N_{Phe}$ means were lower than those of bone collagen (P > 99%) but it is unlikely that feather $\Delta\delta^{15}N_{Glu\text{-}Phe}$ means were higher than those of bone collagen (Table 7a, P = 60%; Fig. 8).

Variation in $\delta^{15}N_{Phe}$ and $\Delta\delta^{15}N_{Glu\text{-}Phe}$ Between Species and Time Periods

Modern Laysan albatross feather had lower $\delta^{15}N_{Phe}$ and higher $\Delta\delta^{15}N_{Glu\text{-}Phe}$ means relative to the Newell's shearwater feather (Table 7b, $P \geq$ 92%; Fig. 7). There was an 81% probability that $\delta^{15}N_{Phe}$ declined in Laysan albatross feather over the past 100 years and only a 47% probability

of a decline for $\Delta\delta^{15}N_{Glu\text{-}Phe}$ (Table 7b; Fig. 8). We did not consider either of these differences to be ecologically or statistically significant.

DISCUSSION

Our comparison of amino acid nitrogen isotope data from feather and collagen reveals that two ecologically distinct species, Newell's shearwater and Laysan albatross, both alter their foraging habits during their annual cycles in a species-specific manner. Furthermore, our data support a trophic decline for Laysan albatross over the past century, a phenomenon that appears to be isolated to a particular season of the annual cycle.

Modern Comparisons

In the case of Newell's shearwater, trophic position during the nonbreeding season is lower than during the breeding season. We are able to ascertain this because the high $\Delta\delta^{15}N_{Glu\text{-}Phe}$ of collagen (year-round data) relative to feather (nonbreeding season data) must derive from the breeding season. The observation that seabirds often feed their chicks different food items than they eat year-round may impose the unique foraging strategy associated with the breeding season (Hodum and Hobson 2000; Le Corre 2003; Cherel 2008; Cherel et al. 2008; Young et al. 2010). If high trophic level prey offer a nutritional benefit, they may be important for satisfying the energetic demands of chick rearing (Gutowsky et al. 2009).

In addition to seasonal trophic differences, chick provisioning may drive seasonal variation in Newell's shearwater foraging location. In comparison to the nonbreeding season, Newell's shearwater $\delta^{15}N_{Phe}$ values indicate a greater reliance on food webs supplied by nitrogen fixation during the breeding season. This may indicate that breeding adults forage extensively in the waters surrounding the Hawaiian Islands, where primary productivity is significantly

supported by nitrogen fixation (Kim et al. 2014). Observational data show Newell's shearwaters less dispersed from Hawaii when they are colony-bound, perhaps to facilitate frequent visits to the burrow (Spear et al. 1995). In contrast, the large variation in nonbreeding season $\delta^{15}N_{Phe}$ values is consistent with dissemination across a broad range that overlaps with a nitrogen isotopic gradient extending east from ^{15}N-enriched waters southeast of Hawaii.

While Newell's shearwaters are year-long residents of the eastern tropical Pacific, Laysan albatross occupy a marine range that encompasses the vast majority of the North Pacific Ocean (BirdLife 2018). However, several tracking studies reveal that Laysan albatross distribution contracts substantially during the early stages of the breeding season, when frequent visits to the colony are required (Fernandez et al. 2001; Hyrenbach et al. 2002; Young 2009; Conners et al. 2015; Gutowsky et al. 2015; Thorne et al. 2015). We considered whether this contracted range could influence Laysan albatross $\Delta\delta^{15}N_{Glu\text{-}Phe}$ data. Laysan albatross that breed in the Hawaiian Islands are atypical among albatrosses in their reliance on tropical waters during the breeding season, where resources are less abundant and patchier than in higher latitudes (Ainley 1977; Seki and Polovina 2001; Conners et al. 2015). Moreover, their constricted breeding season marine range increases the potential for competition (Ashmole 1963; Birt et al. 1987; Schreiber 2001). For example, although Laysan and black-footed albatrosses exhibit spatial segregation at sea for most of the year, during the early breeding season the two species overlap significantly (Fernandez et al. 2001; Fischer et al. 2009; Kappes 2009; Kappes et al. 2010). Perhaps competition in suboptimal low latitudes during an energetically demanding stage of the annual cycle contributes to Laysan albatross relying on lower trophic level prey.

Substantial seasonal differences in the marine distribution of Laysan albatross may explain seasonal variation in nutrient regime use. Laysan albatross $\delta^{15}N_{Phe}$ values are lower in the

nonbreeding season than the yearly average, suggesting a high reliance on waters supported by nitrogen fixation post-breeding. While our understanding of regional variation in nitrogen fixation within the North Pacific Ocean continues to emerge, our data suggest that Laysan albatross are able to access regions of high nitrogen fixation when they are released from their central place foraging strategy and expand their marine range (Shiozaki et al. 2010; Young et al. 2010; Luo et al. 2012).

In addition to illuminating intra-species seasonal foraging differences, our study also permits assessment of inter-species differences in foraging habits within each season. Feather data suggest that, relative to Laysan albatross, Newell's shearwaters occupy a lower trophic position and rely less on food webs supplied by nitrogen fixation during the nonbreeding season. However, during the breeding season, collagen data reveal that both of these relationships are reversed. At this time, Newell's shearwaters appear to occupy a higher trophic position and rely more on food webs supplied by nitrogen fixation than Laysan albatross. Thus, while both species exhibit flexibility in their foraging strategies throughout the annual cycle, this flexibility manifests itself differently in each species and yields inter-species foraging differences that are season-specific. The dynamic relationship between Newell's shearwater and Laysan albatross foraging habits would have escaped notice if we had not analyzed both feather and collagen.

Temporal Comparisons

Flexibility in Laysan albatross foraging strategies may be a particularly beneficial trait given that they appear to have experienced a trophic decline over the past century. Because this trophic decline was evident from collagen but not feather, it seems to be associated solely with the breeding season, which presents unique challenges. Trophic declines have been linked to reproductive decline in other seabirds (Gutowsky et al. 2009). Reproduction is an acutely

energetically expensive phase of the annual cycle when breeders must balance foraging efficiency with rate of energy delivery to the chick (Weimerskirch et al. 2003). Energy requirements may not be fulfilled even if low trophic level prey may have higher energy content than their high trophic level counterparts. If low trophic level prey have a small body size, higher energy content is unlikely to compensate for the increased foraging effort required to catch many smaller organisms in patchy low-latitude waters (Gutowsky et al. 2009). Moreover, catching numerous small prey may contribute to increased trip duration by breeders, which can negatively influence reproductive success (Thorne et al. 2015).

Beyond the potential consequences for Laysan albatross reproduction, the trophic decline we identified has broader implications. As top predators, Laysan albatross act as sentinels of food web dynamics because they integrate trophic information up their food web. Additionally, if their trophic decline is a result of oceanographic change over the past century, any number of marine predators may be similarly affected, an important consideration as we evaluate the consequences of climate change and fisheries on pelagic ecosystems.

Conclusions

Identifying how foraging strategies of two ecologically distinct species—Newell's shearwater and Laysan albatross—differ and vary over a year empowers conservation efforts. Our results imply that management strategies must be tailored to individual species and require addressing threats both on land and at sea. Moreover, because foraging strategies vary over several decades, the ability to look back in time is essential for securing a future for marine species. Laysan albatross appear to be particularly vulnerable to oceanographic change during the breeding season, perhaps because their ability to seek out alternate food sources is hindered. This vulnerability could have severe implications for population viability, especially in various long-

lived, low fecundity species, including Laysan albatross and Newell's shearwater. As humans continue to increase competition with seabirds for food, the ability of marine species to exploit alternative resources will be essential.

APPENDIX

Figure 7. Isotope standard ellipses representing variation in $\delta^{15}N_{Phe}$ and $\Delta\delta^{15}N_{Glu\text{-}Phe}$ (‰) values for modern Newell's shearwater (NESH) and Laysan albatross (LAAL) feather and collagen. Model estimated mean $\delta^{15}N_{Phe}$ and $\Delta\delta^{15}N_{Glu\text{-}Phe}$ values for each population define the center of the ellipse and a covariance matrix determines the shape and orientation. Legend indicates species and tissue type. Time periods and sample sizes (n) follow. NESH: 2013-2016, n = 10 for feather and collagen; LAAL: 2003-2014, n = 10 for feather, n = 11 for collagen.

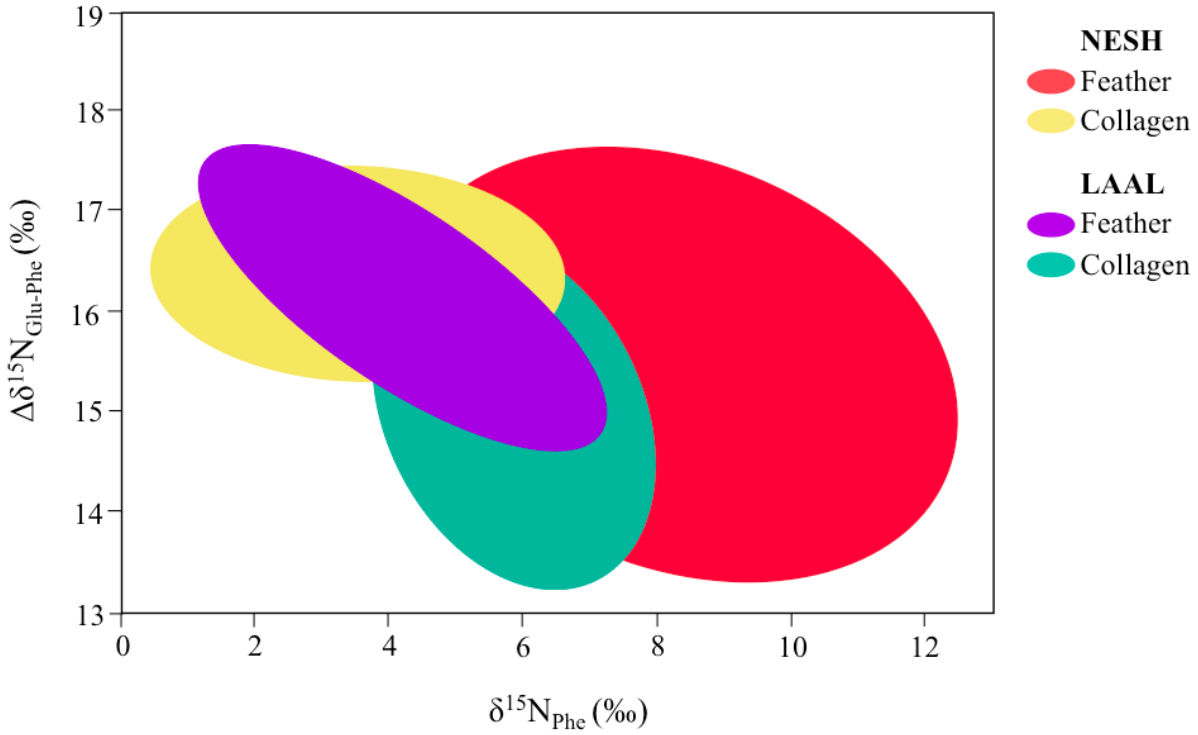

Figure 8. Density distributions of model estimated $\delta^{15}N_{Phe}$ and $\Delta\delta^{15}N_{Glu\text{-}Phe}$ (‰) for Laysan albatross (a) feather and (b) collagen over the past 100 years. Time periods and sample sizes (n) follow: Pre-1950 (1902-1937) n = 9 for feather, n = 11 for collagen; Post-2000 (2003-2014) n = 10 for feather, n = 11 for collagen

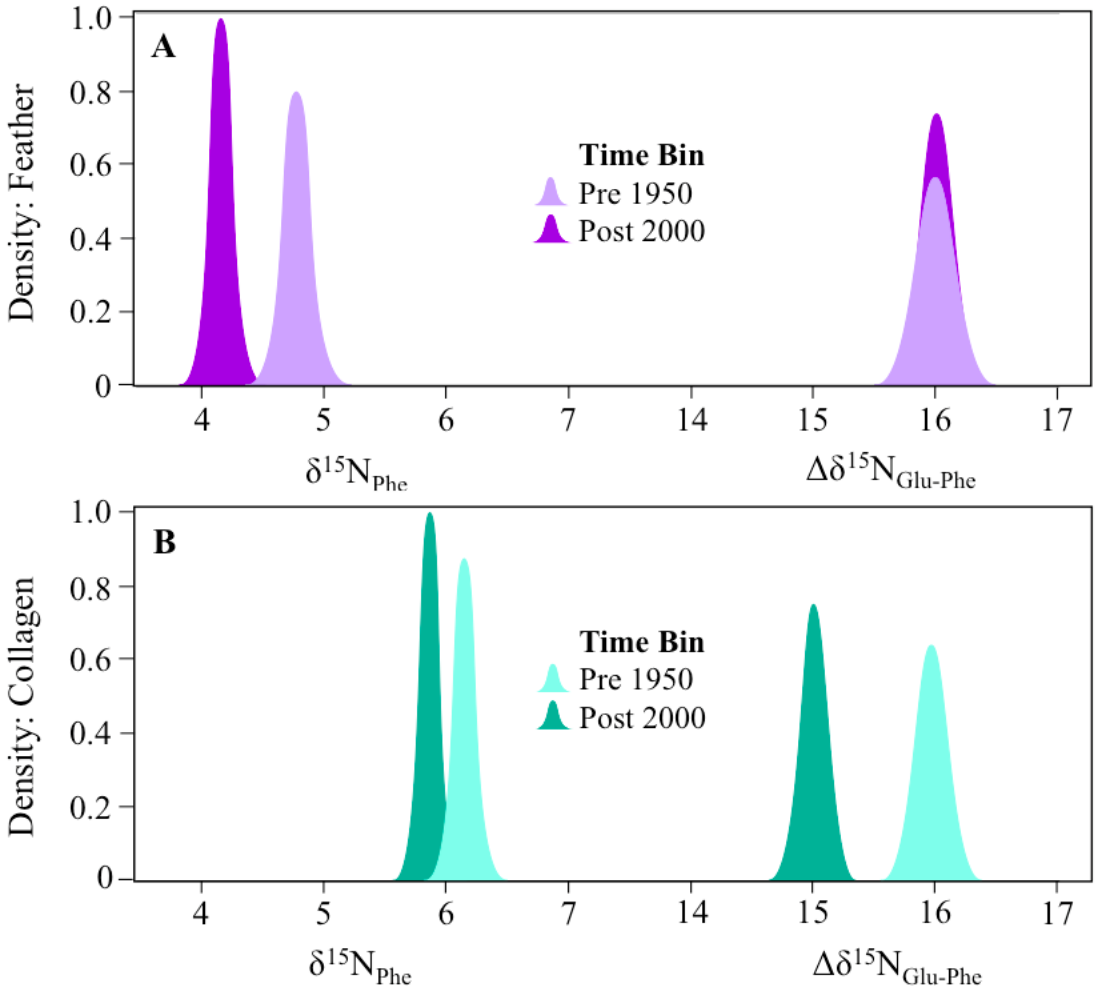

Table 7. Statistical results from hierarchical modeling of feather and collagen isotope data showing variation among populations. Probabilities (*P*) indicate likelihood that $\delta^{15}N_{Phe}$ and $\Delta\delta^{15}N_{Glu\text{-}Phe}$ (‰) are greater in population 1 than in population 2. (a) show tissue type comparisons for Newell's shearwater (NESH) and Laysan albatross (LAAL) data; (b) shows an inter-species comparison between NESH and LAAL, and a temporal comparison for LAAL.

(a)

Population 1 (Feather)	**Population 2 (Collagen)**	***P* Population 1 (Feather) > Population 2 (Collagen)**	
		$\delta^{15}N_{Phe}$ (‰)	**$\Delta\delta^{15}N_{Glu\text{-}Phe}$ (‰)**
NESH (modern)	NESH (modern)	1.00	0.0035
LAAL (modern)	LAAL (modern)	0.0028	0.99
LAAL (historic)	LAAL (historic)	0.0012	0.60

(b)

Population 1	**Population 2**	***P* Population 1 > Population 2**	
		$\delta^{15}N_{Phe}$ (‰)	**$\Delta\delta^{15}N_{Glu\text{-}Phe}$ (‰)**
Mod LAAL feather	Mod NESH feather	0.000033	0.92
Hist LAAL feather	Mod LAAL feather	0.81	0.47

LITERATURE CITED

LITERATURE CITED

Adams J, Flora S. 2010 Correlating seabird movements with ocean winds: linking satellite telemetry with ocean scatterometry. Mar. Biol. 157: 915-929.

Ainley DG, Telfer TC, Reynolds MH. 1997 Newell's Shearwater (*Puffinus newelli*), version 2.0. In: Rodewald PG (ed) The Birds of North America. Cornell Lab of Ornithology, Ithaca, New York, USA.

Ainley DG, Walker WA, Spencer GC, Holmes ND. 2014 The prey of Newell's shearwater *Puffinus newelli* in Hawaiian waters. Mar. Ornithol. 44: 69-72.

Altabet M, Francois R. 1994 Sedimentary nitrogen isotopic ratio as a recorder for surface ocean nitrate utilization. Glob. Biogeochem. Cycles 8: 103-116.

Ashmole NP. 1963 The regulation of numbers of tropical oceanic birds. Ibis 103b: 458-473.

Ballance LT, Ainley DG, Hunt Jr. GL. 2001 Seabird Foraging Ecology. In: Steele JH, Thorpe SA, Turekian KK (eds) Encyclopedia of Ocean Sciences. Academic Press, London, 5: 2636-2644.

Ballance LT, Pitman RL, Fiedler PC. 2006 Oceanographic influences on seabirds and cetaceans of the eastern tropical Pacific: a review. Prog. Oceanogr. 69: 360-390.

BirdLife International. 2018 IUCN Red List for birds. Downloaded from http://www.birdlife.org on 1/12/2018.

Birt VL, Birt TP, Goulet D, Carins DK, Montevecchi WA. 1987 Ashmole's halo: direct evidence for prey depletion by a seabird. Mar. Ecol. Progr. Ser. 40: 205-208.

Blanke CM, Chikaraishi Y, Takizawa Y, Steffan SA, Dharampal PS, Vander Zanden MJ. 2017 Comparing compound-specific and bulk stable nitrogen isotope trophic discrimination factors across multiple freshwater fish species and diets. Can. J. Fish. Aquat. 74: 1291-1297.

Broughton JM. 1994 Size of the bursa of Fabricius in relation to gonad size and age in Laysan and Black-footed Albatrosses. Condor 96: 203-207.

Casciotti KL, Trull TW, Glover DM, Davies D. 2008 Constraints on nitrogen cycling at the subtropical North Pacific Station ALOHA from isotopic measurements of nitrate and particulate nitrogen. Deep. Res. Part II: Trop. Stud. Oceanogr. 55: 1661-1672.

Cherel Y. 2008. Isotopic niches of emperor and Adélie penguins in Adélie Land, Antarctica. Mar. Biol. 154: 813-821.

Cherel Y, Le Corre M, Jaquemet S, Menard F, Richard P, Weimerskirch H. 2008 Resource partitioning within a tropical seabird community: new information from stable isotopes. Mar. Ecol. Prog. Ser. 366: 281-291.

Chikaraishi Y, Kashiyama Y, Ogawa NO, Kitazato H, Ohkouchi N. 2007 Metabolic control of nitrogen isotope composition of amino acids in macroalgae and gastropods: implications for aquatic food web studies. Mar. Ecol. Prog. Ser. 342: 85-90.

Chikaraishi Y, Ogawa NO, Kashiyama Y, Takano Y, Suga H, Tomitani A, Miyashita H, Kitazato H, Ohkouchi N. 2009 Determination of aquatic food- web structure based on compound-specific nitrogen isotopic composition of amino acids. Limnol. Oceanogr: Methods 7: 740-750.

Chikaraishi Y, Steffan SA, Ogawa NO, Ishikawa NF, Sasaki Y, Tsuchiya M, Ohkouchi N. 2014 High-resolution food webs based on nitrogen isotopic composition of amino acids. Ecol. Evol. 4: 2423-2449.

Conners MG, Hazen EL, Costa DP, Shaffer SA. 2015 Shadowed by scale: subtle behavioral niche partitioning in two sympatric, tropical breeding albatross species. Mov. Ecol. 3: 28.

Cook TR, Lescroel A, Cherel Y, Kato A, Bost C-A. 2013 Can foraging ecology drive the evolution of body size in a diving endotherm? PLoS One 8: e56297.

Edwards AE, Rohwer S. 2005 Large-scale patterns of molt activation in the flight feathers of two albatross species. Condor 107: 835-848.

Edwards AE, Fitzgerald SM, Parrish JK, Klavitter JL, Romano MD. 2015 Foraging strategies of Laysan albatross inferred from stable isotopes: implications for association with fisheries. PLoS One 10: e0133471.

Farmer RG, Leonard ML. 2011 Long-term feeding ecology of Great Black-backed Gulls (*Larus marinus*) in the northwest Atlantic: 110 years of feather isotope data. Can. J. Zool. 89: 123-133.

Fernández P, Anderson DJ, Sievert PR, Huyvaert KP. 2001 Foraging destinations of three low-latitude albatross (Phoebastria) species. J. Zool. 254: 391-404.

Fischer KN, Suryan RM, Roby DD, Balogh GR. 2009 Post-breeding season distribution of black-footed and Laysan albatrosses satellite-tagged in Alaska: inter-specific differences in spatial overlap with North Pacific fisheries. Biol. Conserv. 142: 751-760.

Gagne TO, Hyrenbach KD, Hagemann ME, Van Houtan KS. 2018 Trophic signatures of seabirds suggest shifts in oceanic ecosystems. Sci. Adv. 4: eaao3946.

Gelman A, Hill J. 2007 Data analysis using regression and multilevel/hierarchical models. Cambridge University Press, New York, USA.

Graham BS, Koch PL, Newsome SD, McMahon KW, Aurioles D. 2010 Using isoscapes to trace the movements and foraging behavior of top predators in oceanic ecosystems. In: West JB, Bowen GJ, Dawson TE, Tu KP (eds) Isoscapes: Understanding Movement, Pattern, and Process on Earth Through Isotope Mapping. Springer Science, Dordrecht, The Netherlands, pp 299-318.

Gutowsky SE, Janssen MH, Arcese P, Kyser TK, Ethier D, Wunder MB, Bertram DF, Tranquilla LM, Lougheed C, Norris DR. 2009 Concurrent declines in nestling diet quality and reproductive success of a threatened seabird over 150 years. Endanger. Species Res. 15: 247-254.

Gutowsky SE, Leonard ML, Conners MG, Shaffer SA, Jonsen ID. 2015 Individual-level variation and higher-level interpretations of space use in wide-ranging species: an albatross case study of sampling effects. Front. Mar. Sci. 2: 93.

Harrison CS, Hida TS, Seki MP. 1983 Hawaiian seabird feeding ecology. Wildl. Monogr. 85: 3-71.

Hebert CE, Popp BN, Fernie KJ, Ka'apu-Lyons C, Rattner BA, Wallsgrove N. 2016 Amino acid specific stable nitrogen isotope values in avian tissues: insights from captive American Kestrels and wild Herring Gulls. Environ. Sci. Technol. 50: 12928-12937.

Hinke JT, Polito MJ, Goebel ME, Jarvis S, Reiss CS, Thorrold SR, Watters GM. 2015 Spatial and isotopic niche partitioning during winter in chinstrap and Adélie penguins from the South Shetland Islands. Ecosphere. 6: 1-32.

Hodum PJ, Hobson KA. 2000 Trophic relationships among Antarctic fulmarine petrels: insights into dietary overlap and chick provisioning strategies inferred from stable-isotope ($\delta^{15}N$ and $\delta^{13}C$) analyses. Mar. Ecol. Prog. Ser. 198: 273-281.

Hyrenbach KD, Fernández P, Anderson DJ. 2002 Oceanographic habitats of two sympatric North Pacific albatrosses during the breeding season. Mar. Ecol. Prog. Ser. 233: 283-301.

Jackson AL, Inger R, Parnell AC, Bearhop S. 2011 Comparing isotopic niche widths among and within communities: SIBER—Stable Isotope Bayesian Ellipses. R. J. Anim. Ecol. 80: 595-602.

Jaeger A, Jaquemet S, Phillips RA, Wanless RM, Richard P, Cherel Y. 2013 Stable isotopes document inter-and intra-specific variation in feeding ecology of nine large southern Procellariiformes. Mar. Ecol. Prog. Ser. 490: 255-266.

Kappes M. 2009 Comparative foraging ecology and energetics of albatrosses, PhD dissertation, University of California, Santa Cruz, California, USA.

Kappes MA, Shaffer SA, Tremblay Y, Foley DG, Palacios DM, Robinson PW, Bograd SJ, Costa DP. 2010 Hawaiian albatrosses track interannual variability of marine habitats in

the North Pacific. Prog. Oceanogr. 86: 246-260.

Karl D, Letelier R, Tupas L, Dore J, Christian J, Hebel D. 1997 The role of nitrogen fixation in biogeochemical cycling in the subtropical North Pacific Ocean. Nature 388: 533-538.

Kim IN, Lee K, Gruber N, Karl DM, Bullister JL, Yang S, Kim TW. 2014 Increasing anthropogenic nitrogen in the North Pacific Ocean. Science 346: 1102-1106.

Langston NE, Rohwer S. 1996 Molt-breeding tradeoffs in albatrosses: life history implications for big birds. Oikos 76: 498-510.

Le Corre M, Cherel Y, Lagarde F, Lormée H, Jouventin P. 2003 Seasonal and inter-annual variation in the feeding ecology of a tropical oceanic seabird, the red-tailed tropicbird Phaethon rubricauda. Mar. Ecol. Prog. Ser. 255: 289-301.

Lewison R *et al.* 2012 Research priorities for seabirds: improving seabird conservation and management in the 21st century. Endanger. Species Res. 17: 93-121.

Luo YW *et al.* 2012 Database of diazotrophs in global ocean: Abundance, biomass, and nitrogen fixation rates. Earth Syst. Sci. Data 4: 47-73.

McCarthy MD, Benner R, Lee C, Fogel ML. 2007 Amino acid nitrogen isotopic fractionation patterns as indicators of heterotrophy in plankton, particulate, and dissolved organic matter. Geochim. Cosmochim. Acta 71: 4727-2744.

McClelland JW, Montoya JP. 2002 Trophic relationships and the nitrogen isotopic composition of amino acids in plankton. Ecol. 83: 2173-2180.

McMahon KW, McCarthy, MD. 2016 Embracing variability in amino acid $\delta^{15}N$ fractionation: mechanisms, implications, and applications for trophic ecology. Ecosphere 7: e01511.

Minagawa M, Wada E. 1984 Stepwise enrichment of ^{15}N along food chains: further evidence and the relation between $\delta^{15}N$ and animal age. Geochim. Cosmochim. Acta 48: 1135-1140.

Ohkouchi N *et al.* 2017 Advances in the application of amino acid nitrogen isotopic analysis in ecological and biogeochemical studies. Org. Geochem. 113: 150-174.

Ostrom PH, Wiley AE, James HF, Rossman S, Walker WA, Zipkin EF, Chikaraishi Y. 2017 Broad-scale trophic shift in the pelagic North Pacific revealed by an oceanic seabird. Proc. R. Soc. B. 284: 20162436-20162442.

Plummer M. 2003 JAGS: a program for analysis of Bayesian graphical models using Gibbs Sampling. Proceedings of the Third International Workshop on Distributed Statistical Computing. R Project for Statistical Computing, Vienna, Austria.

Popp BN, Graham BS, Olson RJ, Hannides CCS, Lorr MJ, Lopez-Ibarra G, Galvan-Magana F, Fry B. 2007 Insight into the trophic ecology of yellowfin tuna, *Thunnus albacares*, from compound specific nitrogen isotope analysis of proteinaceous amino acids. In: Dawson TE, Siegwolf RTW (eds) Stable isotopes as indicators of ecological change. Elsevier, New York, USA, pp 173-190.

Pyle P. 2008 Molt and age determination in Procellariiformes. In: Identification Guide to North American Birds, Part 2. Slate Creek Press, Point Reyes Station, California, USA, pp 248-260.

R Development Core Team. 2013 R: a language and environment for statistical computing. R Foundation for Statistical Computing, Vienna, Austria.

Rossman S, Ostrom PH, Stolen M, Barros NB, Gandhi H, Stricker CA, Wells RS. 2015 Individual specialization in the foraging habits of female bottlenose dolphins living in a trophically diverse and habitat rich estuary. Oecologia 178: 415-425.

Rossman S, Ostrom PH, Gordon F, Zipkin EF. 2016 Beyond carbon and nitrogen: guidelines for estimating three-dimensional isotopic niche space. Ecol. Evol. 6: 2405-2413.

Rucklidge GJ, Milne G, McGaw BA, Milne E, Robins SP. 1992 Turnover rates of different collagen types measured by isotope ratio mass spectrometry. Biochim. Biophys. Acta 1156: 57-61.

Schreiber EA, Burger J. 2001 Biology of marine birds. CRC Press, Florida, USA.

Seki M, Polovina J. 2001 Biological enhancement at cyclonic eddies tracked with GOES thermal imagery in Hawaiian waters. Geophys. Res. Lett. 28: 1583-1586.

Shiozaki T, Furuya K, Kodama T, Kitajima S, Takeda S, Takemura T, Kanda J. 2010 New estimation of N_2 fixation in the western and central Pacific Ocean and its marginal seas. Glob. Biogeochem. Cycles 24: GB1015.

Sigman DM, Mccorkle DC, Francois R, Fischer G. 2000 The $\delta^{15}N$ of nitrate in the Southern Ocean: nitrogen cycling and circulation in the ocean interior. J. Geophys. Res. 105: 19599-19614.

Spear LB, Ainley DG, Nur N, Howell SNG. 1995 Population size and factors affecting at-sea distributions of four endangered Procellariids in the tropical Pacific. Condor 97: 613-638.

Thorne LH, Hazen EL, Bograd SJ, Foley DG, Conners MG, Kappes MA, Kim HM, Costa DP, Tremblay Y, Shaffer SA. 2015 Foraging behavior links climate variability and reproduction in North Pacific albatrosses. Mov. Ecol. 3: 27.

Warham J. 1996 The behavior, population biology and physiology of the petrels. Academic Press, University of Canterbury, Christchurch, New Zealand.

Weimerskirch H, Ancel A, Caloin M, Zahariev A, Spagiari J, Kersten M, Chastel O. 2003 Foraging efficiency and adjustment of energy expenditure in a pelagic seabird provisioning its chick. J. Anim. Ecol. 72: 500-508.

Wiley AE, Ostrom PH, Stricker CA, James HF, Gandhi HF. 2010 Isotopic characterization of flight feathers in two pelagic seabirds: Sampling strategies for ecological studies. Condor 112: 337-346.

Wiley AE, Welch AJ, Ostrom PH, James HF, Stricker CA, Fleischer RC, Gandhi H, Adams J, Ainley DG, Duvall F, Holmes N. 2012 Foraging segregation and genetic divergence between geographically proximate colonies of a highly mobile seabird. Oecologia 168: 119-130.

Wiley AE *et al.* 2013 Millennial-scale isotope records from a wide-ranging predator show evidence of recent human impact to oceanic food webs. Proc. Natl. Acad. Sci. 110: 8972-8977.

Young LC. 2009 Foraging ecology, population genetics and risk of fisheries bycatch for the Laysan albatross (*Phoebastria immutabilis*). PhD dissertation, University of Hawaii, Hawaii, USA.

Young HS, McCauley DJ, Dirzo R, Dunbar RD, Shaffer SA. 2010 Niche partitioning among and within sympatric tropical seabirds revealed by stable isotope analysis. Mar. Ecol. Prog. Ser. 416: 285-294.